Reconfigurable Intelligent Surfaces-Assisted Secure Wireless Communication in Wiretap Systems with Multiple Base Stations

Feihong Chen, Fengqian Guo, Yuang Chen, Hancheng Lu, *Senior Member, IEEE*

***Abstract*— In this paper, we consider a multi-RIS-assisted multi-BS and multi-user wiretap system with malicious eavesdroppers in hotspots. To suppress the behavior of eavesdroppers and achieve secure communication with high secrecy rate (SR) for as many legitimate users as possible, the secure BSs-users association is essential for multi-BS. Since the introduction of RISs extends BSs signal coverage, providing more access possibilities for each BS to associate with potential users, the mutual impact of passive beamforming (PBF) at RISs and secure BSs-users association should be considered together. Therefore, we formulate a sum secrecy rate (SSR) maximization problem by jointly optimizing transmit beamforming (TBF) at BSs, PBF at RISs, and secure BSs-users association. To tackle such non-convex problem, we decompose it into three subproblems and solved them through alternating optimization. The TBF subproblem is efficiently solved by performing successive convex approximation and semi-definite relaxation methods. And the PBF subproblem is tackled utilizing the quadratic transform approach. Meanwhile, we handle the secure BSs-users association subproblem with auction theory. Simulation results demonstrate the proposed algorithm can achieve higher system SSR and SR for each user compared to baselines, which further emphasizes the effectiveness of jointly considering the PBF at RISs and secure user association in enhancing system security in the multi-BS wiretap system.**

***Index Terms*— Reconfigurable intelligent surface (RIS), beamforming, secure association, physical layer security, secrecy rate.**

I. Introduction

In recent years, with the explosive growth of traffic demand, there has been a dramatic increase in the number of terminal devices. For upcoming sixth generation (6G) mobile communication and beyond, wireless communication networks will need to support massive devices and achieve a capacity demand of 1000x [1] [2]. To fulfill the high data rate demands of multiple terminal users as well as achieve timely and efficient communication, deploying multiple base stations (BSs) in some hotspots such as shopping malls and stadiums to enhance the communication quality has significant importance.

However, due to the broadcast nature of wireless channels, signal leakage inevitably occurs when BSs communicate with users. Consequently, malicious eavesdroppers can easily capture confidential message sent to legitimate users, which will reduce the security performance of the system. From an information theory standpoint, physical layer security (PLS) has been widely investigated to guarantee secure wireless communication [3]. Serving as a supplement to encryption techniques in the network layer, PLS enhancement techniques typically take some security metrics like secrecy rate (SR) and secrecy outage probability (SOP) into consideration to achieve secure communication, which does not rely on secret keys. By fully utilizing differences between links of legitimate users and eavesdroppers, the information illegally captured by eavesdroppers can be effectively restricted. Nevertheless, with the increase in the number of antennas, BSs and users, traditional PLS enhancement techniques such as artificial noise (AN), cooperative jamming, and relaying, are becoming increasingly unable to meet the requirements of green communication. Besides, the security performance of these techniques is limited to some extent especially when the channel conditions are unfavorable. Therefore, it is highly necessary to find a more energy-efficient and flexible technology to improve the communication quality and security performance of wireless communication systems.

Benefited from the rapid development of electromagnetic metasurface technology, reconfigurable intelligent surface (RIS), also referred to intelligent reflecting surface (IRS), as a promising technology in future wireless communication, has attracted extensive interest from both academia and industry [4]. RIS is essentially a planar structure comprising a multitude of low-cost passive reflecting elements, which can be meticulously designed to manipulate the phase and amplitude of the incident signal. As a consequence, the signal can be directed towards a desired direction, resulting in the effect of passive beamforming (PBF). Due to its capability to reshape wireless channels with low cost and energy consumption, RIS-enhanced wireless communication has captured widespread concern [5]–[8]. In [5], a typical RIS-aided multiple-input single-output (MISO) communication system with multiple users is investigated. By jointly optimizing the transmit beamforming (TBF) at the BS and PBF at the RIS, the achievable rate and signal coverage of the system are significantly improved compared to the wireless systems without RIS. The authors in [6] further studied the energy efficiency (EE) optimization problem in a similar scenario and demonstrated RIS-enhanced communication can provide up to 300% higher EE than the relay-assisted one. In [7], the

This work was supported by National Key R&D Program of China under Grant 2020YFA0711400, and National Science Foundation of China under Grant U21A20452.

F. Chen, F. Guo, Y. Chen, H. Lu are with the Information Network Laboratory, Department of Electronic Engineering and Information Science, University of Science and Technology of China, Hefei 230027, China (e-mail: chenfeihong@mail.ustc.edu.cn; fqguo@ustc.edu.cn; yuangchen21@mail.ustc.edu.cn; hclu@ustc.edu.cn).

authors investigated a RIS-assisted multi-user MISO system under residual hardware impairments and correlated Rayleigh fading. A closed-form expression for spectral efficiency was derived, and a low-complexity RIS beamforming method was proposed based on large-scale statistics, significantly reducing computational cost. And authors in [8] investigated a RIS-aided millimeter wave (mmWave) multiple-input multiple-output (MIMO) system, demonstrating the effectiveness of RIS in greatly enhancing mmWave communication. Besides, RIS-assisted some novel scenarios such as movable antenna (MA) systems [9], cell-free networks [10], [11] and internet of video things (IoVT) systems [12] were investigated respectively, which further shows the compatibility of RIS with existing communication systems. In [9], the authors introduced an active RIS-assisted MA system to overcome capacity limitations in multi-scatterer environments. By jointly optimizing BS beamforming, RIS phase shifts, and MA positioning, the proposed approach significantly improves the sum-rate performance over traditional fixed antenna systems. In particular, [10] studied hybrid beamforming design for RIS-aided full-duplex cell-free networks, proposing an efficient iterative algorithm to jointly optimize digital and analog beamformers, RIS phase shifts and uplink power, demonstrating significant performance gains over baseline schemes. And in [12], a multi-RIS aided IoVT system was proposed to reduce long-term power consumption under delay constraints. By jointly optimizing power control and RIS beamforming using Lyapunov and alternating optimization techniques, the system achieves superior energy efficiency compared to benchmark schemes.

Owing to the remarkable potential of RIS in enhancing system communication performance, as well as its low cost and low power consumption, RIS-assisted secure communication systems have gained increasing attention recently. One important research direction is to enhance the PLS performance of wireless systems by deploying and optimizing the phase shifts of RIS in a reasonable way. By utilizing the PBF effect brought by RIS, the signal can exhibit coherent superposition in desired users and incoherent superposition in malicious eavesdroppers, which can effectively suppress the signal leakage caused by eavesdroppers. Existing related research mainly focuses on RIS-assisted PLS enhancement in a single BS scenario [13]–[23]. In [13], a RIS-aided MISO wiretap system with one eavesdropper was investigated, where the TBF at BS and PBF of RIS were jointly optimized by the alternating method to maximize the system SR. Simulation results indicated that introducing RIS can notably improve system security performance. Further, authors in [14] confirmed the effectiveness of combining RIS with traditional AN technique in enhancing system PLS. And [15] studied a more general RIS-aided MISO wiretap system with multiple users and eavesdroppers, where the minimum SR maximization problem was solved. In [16], multiple RISs were deployed to guarantee the secure communication in the presence of multiple eavesdroppers with multiple antennas. The joint design of the TBF, AN covariance matrix at the BS, and PBF of RISs were considered to maximize the system sum rate under security constraints. As for the more complicated RIS-assisted MIMO wiretap system, authors in [17] jointly optimized the transmit precoding matrix, AN transmit covariance matrix at BS, and PBF of RIS to ensure secure communication. The same scenario was investigated in [18], where the system SR was improved under the full CSI and unknown CSI of the eavesdropper. Furthermore, authors in [19] focused on the RIS-enhanced multi-carrier MIMO wiretap system and maximized the system SR. Apart from these conventional wiretap scenarios, RIS can also be applied in some emerging communication scenarios. In [20], RIS was utilized to enhance PLS in the unmanned aerial vehicles (UAV) system. By jointly optimizing the beamforming and UAV trajectory, the average SR is maximized. And authors in [21] introduced RIS into an integrated sensing and communication wiretap system, where the deep reinforcement learning method is adopted to improve the system SR. In [22], RIS was employed in a cognitive radio network to jointly enhance spectrum sensing and secrecy performance. A block coordinate descent-based algorithm was proposed to optimize beamforming and RIS phase shifts, improving both sensing accuracy and secrecy rate under perfect and imperfect CSI scenarios. And in [23], the authors investigated RIS-assisted near-field secure non-orthogonal multiple access systems with untrusted users, and proposed an alternating optimization algorithm to jointly design RIS beamforming and power allocation, demonstrating the benefits of near-field beam focusing for enhancing security and fairness trade-offs.

The aforementioned studies [13]–[23] clearly demonstrate the effectiveness of RIS in enhancing the PLS of the single BS wiretap system. However, the PLS performance of introducing RIS into multi-BS wiretap scenarios has not been thoroughly investigated. In contrast to a single BS system, a multi-BS system introduces additional consideration into the BSs-users association [24]–[28] problem. The interaction between RIS and BSs-users association prevents existing optimization frameworks from being directly applied to our proposed RIS-assisted multi-BS wiretap systems. By establishing appropriate BSs-users associations in a multi-BS system, it is possible to reduce interference between users, increase system capacity, and achieve load balancing among BSs. Furthermore, in the presence of malicious eavesdroppers, if BSs are randomly selected to communicate with users, severe signal leakage may occur. The proper BSs-users association can help limit the wiretapping of eavesdroppers, guaranteeing secure communication for more users. For RISs-assisted multi-BS and multi-user wiretap scenario, we need to consider the non-convex cooperation problem of RISs, multi-BS, and multi-user together to enhance the system PLS, which exhibits strong coupling relationship and is hard to solve. On one hand, the introduction of RISs creates additional reflected line-of-sight (LOS) links, extending the signal coverage and providing more possibilities for secure association between BSs and users. By fully leveraging the capability of RISs in reshaping wireless channels, it becomes more flexible to associate BSs with legitimate users, especially for users previously unable to be well served by some BSs. Therefore, the impact of both RISs and secure BSs-users association should be investigated together. On the other hand, since RISs are introduced into the system to reflect confidential signals, while enhancing the communication quality of legitimate users, it may also

result in the eavesdroppers receiving more signals. Hence, it is necessary to properly design the PBF at RISs, so that the signal can be enhanced at users while weakened at the eavesdroppers, effectively decreasing the wiretapping rate. Meanwhile, how to design active TBF for users served by the selected BS to interfere with the eavesdroppers is also an issue we need to focus on, which further couples the optimization problem.

To tackle the aforementioned challenge, in this paper, we study the security performance of a multi-RIS-assisted multi-BS multi-user wiretap system with malicious eavesdroppers. The following summarizes our main contributions:

1) We propose a multi-RIS-aided multi-BS multi-user wiretap system in hotspots where high demand for data is required and the possibility of signal leakage caused by malicious eavesdroppers is high. To ensure secure wireless communication as much as possible, the BSs-users association needs to be elaborately designed to counteract the eavesdroppers. Simultaneously, RISs are properly deployed to extend the signal coverage of each BS and provide more selectivity for the secure BSs-users association.

2) Under the proposed wiretap system, we formulate a sum SR maximization based on secure user association (SSRM-SUA) problem. We intend to optimize the TBF at BSs, the PBF at RISs, and the secure BSs-users association together to achieve secure communication with high SR for as many users as possible. Due to the non-convexity of the proposed SSRM-SUA problem, it is hard to obtain the optimal solution. Hence, we adopt the alternating optimization (AO) method to decompose the original problem into three subproblems: TBF optimization subproblem with given PBF of RISs and secure BSs-users association, PBF optimization subproblem with given TBF at BSs and secure BSs-users association, secure BSs-users association optimization subproblem with given TBF at BSs and PBF of RISs.

3) To solve the non-convex TBF optimization subproblem, we first adopt successive convex approximation (SCA) and semi-definite relaxation (SDR) techniques to transform it into convex problem and prove the optimal solution is always rank-one, which can be efficiently obtained. For the non-convex PBF optimization subproblem, a series of mathematical approximations and manipulations are first made to transform it into quadratic form and then each reflecting element of RIS is iteratively optimized with other elements fixed. As for the secure BSs-users association optimization subproblem, we propose the two-step secure association algorithm based on auction theory to efficiently associate BSs with users.

4) Finally, we thoroughly analyze whether the introduction of RISs and secure BSs-users association can improve system security with different baselines. Simulation results indicate that the proposed algorithm outperforms baselines with respect to system SSR and SR for each user, which mainly attributed to the appropriate joint design of TBF at BSs, PBF at RISs and secure BSs-users association, effectively harnessing the communication potential of the multi-BS system and suppressing malicious eavesdroppers.

The rest of this paper is organized as follows. In Section II, we describe the proposed multi-RIS-aided multi-BS multi-user wiretap system and propose the SSRM-SUA optimization problem. In Section III, the optimization problem is analyzed and solved. Simulation results demonstrate the effectiveness of the proposed algorithm in Section IV. Finally, we conclude this paper in Section V.

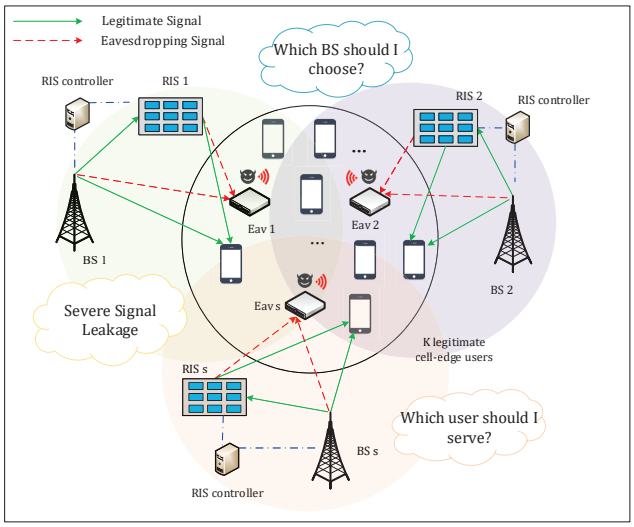

Fig. 1. Proposed multi-RIS-assisted multi-BS multi-user wiretap system.

Notations: We denote scalars, vectors, and matrices as italic, bold lower-case, and bold upper-case letters, respectively. $\mathbb{R}^{x\times y}$ and $\mathbb{C}^{x\times y}$ represent $x \times y$ real-valued space and complex-valued matrices, separately. $(*)^T$ and $(*)^H$ represent the transpose and conjugate transpose operators, respectively. $\arg(*)$ denotes the phase extraction operator and $\mathrm{diag}(*)$ is the diagonalization operator. $\|\cdot\|_0$ and $\|\cdot\|_F$ means the ℓ_0 and Frobenius norm, respectively. $[*]^+$ denotes the non-negative operator, namely $\max\{*, 0\}$.

II. System Model and Problem Formulation

A. Multi-RIS-assisted multi-BS multi-user wiretap system

In hotspots where user traffic demands are high, total S BSs are deployed strategically to meet communication needs for K users. However, due to the presence of malicious and powerful eavesdroppers around each BS, the confidential information transmitted from BSs to legitimate users has suffered from severe signal leakage. Under such a scenario, ensuring secure communication between BSs and users becomes a crucial concern. BSs and users need to determine the corresponding association while considering security as a prerequisite. To further enhance signal coverage (especially for cell-edge users) and effectively suppress eavesdropping (passive secure beamforming), total L low-cost RISs are separately deployed near each BS to provide more options for BSs-users association, thus achieving secure communication as much as possible. The proposed overall communication system is illustrated in Fig.1. Here, RISs can reflect signals from assisted-BS to served users and the eavesdropper around BS s can also receive the reflected signals. Specifically, each RIS is equipped with a micro-embedded controller which can receive control signals from BS to adjust the phase and amplitude of its own elements. For convenience, the sets of the user indexes, BS indexes, and RIS indexes are denoted as $\mathcal{K} = \{1, 2, \cdots, K\}$, $\mathcal{S} = \{1, 2, \cdots, S\}$ and $\mathcal{L} = \{1, 2, \cdots, L\}$, respectively.

Moreover, each BS is equipped with M antennas, arranged in the form of uniform planar array (UPA). Both legitimate users and eavesdroppers in the system are equipped with a single antenna. In addition, the number of passive reflecting elements of each RIS is N and UPA is also adopted. We define the reflection coefficient matrix of the l-th RIS as $\boldsymbol{\Psi}_l = \text{diag}\{\varrho_{l,1}e^{j\theta_{l,1}}, \cdots, \varrho_{l,N}e^{j\theta_{l,N}}\} \in \mathbb{C}^{N\times N}$, where $\varrho_{l,n} \in [0,1]$, $\theta_{l,n} \in [0, 2\pi)$ represent the amplitude and phase shift of the n-th element at the l-th RIS, respectively. Generally, the reflection coefficient of RIS is designed to maximize signal reflection, i.e., total reflection. Hence, we assume the amplitude reflection coefficient $\varrho_{l,n} = 1, \forall l \in \mathcal{L}$, $\forall n = 1, 2, \cdots, N$ in this paper. Considering that the signal reflected by the RIS is subject to distance product and higher path loss, the power of signals reflected twice or more by the RIS can be neglected [5]. In practice, the reflecting elements of RIS only have finite reflection levels. Therefore, we consider discrete phase shift at each element of the l-th RIS and the phase shifts of the l-th RIS can be defined as

$$\theta_{l,n} \in \mathcal{F} \triangleq \left\{0, \frac{2\pi}{2^b}, \frac{2\pi * 2}{2^b}, ..., \frac{2\pi * (2^b - 1)}{2^b}\right\}, \forall l \in \mathcal{L}, \quad (1)$$

where b represents the number of bits of quantized levels.

Since multiple BSs are deployed in the system to support multi-user communication, considering the severe signal leakage caused by malicious eavesdroppers, it is crucial to assign appropriate BSs for users. The allocation of BSs needs to consider two factors comprehensively. On one side, when allocating BSs, it is necessary to ensure secure communication for users as much as possible, i.e., reducing signal leakage. On the other side, the deployment of multiple BSs incurs certain costs and interference inevitably. To maximize the utilization of the system, each BS should serve at least one user, which can effectively avoid BS underload or overload. Additionally, each user can only be served by one BS simultaneously to reduce interference. Based on this, we further define the BSs-users association matrix $\mathcal{B} \in \mathbb{R}^{S\times K}$ as

$$\mathcal{B} = [\boldsymbol{b}_1, \boldsymbol{b}_2, \cdots, \boldsymbol{b}_K] = \begin{bmatrix} \underbrace{b_{1,1}, b_{1,2}, \cdots, b_{1,K}}_{\widetilde{\boldsymbol{b}}_1} \\ \underbrace{b_{2,1}, b_{2,2}, \cdots, b_{2,K}}_{\widetilde{\boldsymbol{b}}_2} \\ \vdots \\ \underbrace{b_{S,1}, b_{S,2}, \cdots, b_{S,K}}_{\widetilde{\boldsymbol{b}}_S} \end{bmatrix}, \quad (2)$$

where $\boldsymbol{b}_k = [b_{1,k}, b_{2,k}, \cdots, b_{S,k}]^T \in \mathbb{R}^{S\times 1}$ is the association vector for the k-th user, indicating which BS is allocated to serve the k-th user. And $\widetilde{\boldsymbol{b}}_s$ is the association vector for the s-th BS, representing which users are served by the s-th BS. The binary decision variable $b_{s,k} \in \{0,1\}, \forall s \in \mathcal{S}, \forall k \in \mathcal{K}$ denotes the connection status between the corresponding BS and user. If $b_{s,k} = 1$, the k-th user is connected to the s-th BS and if $b_{s,k} = 0$, the k-th user terminates communication with the s-th BS. Once the association vector $\boldsymbol{b}_k$ for the k-th user is configured, the specific eavesdropper around BS s can follow the association result to wiretap the k-th user served by the s-th BS. Therefore, based on the association variables $b_{s,k}$, it is indispensable to determine which BS is allocated to the k-th user to alleviate the wiretapping from eavesdroppers.

B. Downlink transmissions wiretap model

In our considered system, since total L RISs are deployed to enhance communication, additional reflected LOS links are introduced. As for legitimate users, we define the equivalent channel between the s-th BS and the k-th user as $\boldsymbol{h}_{s,k}^H \in \mathbb{C}^{1\times M}$, which is composed of the direct link between the s-th BS and the k-th user as well as the reflected link brought by the corresponding RIS :

$$\boldsymbol{h}_{s,k}^H = \underbrace{\boldsymbol{h}_{d,s,k}^H}_{\text{BS-user}} + \underbrace{\boldsymbol{h}_{l,k}^H \boldsymbol{\Psi}_l \boldsymbol{G}_{s,l}}_{\text{BS-RIS-user}}, \quad (3)$$

where $\boldsymbol{h}_{d,s,k}^H \in \mathbb{C}^{1\times M}$ denotes the baseband equivalent channel of the direct link between the s-th BS and the k-th user, $\boldsymbol{h}_{l,k}^H \in \mathbb{C}^{1\times N}$ denotes the channel matrix of the l-th RIS to the k-th user link and $\boldsymbol{G}_{s,l} \in \mathbb{C}^{N\times M}$ is the channel matrix of the s-th BS to the l-th RIS link. As for the malicious eavesdropper monitoring BS s, the equivalent channel between the s-th BS and the eavesdropper is denoted as $\boldsymbol{h}_{s,e}^H \in \mathbb{C}^{1\times M}$, which has a similar expression format to $\boldsymbol{h}_{s,k}^H$ as the following:

$$\boldsymbol{h}_{s,e}^H = \underbrace{\boldsymbol{h}_{de,s}^H}_{\text{BS-Eav}} + \underbrace{\boldsymbol{h}_{l,e}^H \boldsymbol{\Psi}_l \boldsymbol{G}_{s,l}}_{\text{BS-RIS-Eav}}, \quad (4)$$

where $\boldsymbol{h}_{de,s}^H \in \mathbb{C}^{1\times M}$ denotes the baseband equivalent channel of the direct link between the s-th BS and the around eavesdropper, $\boldsymbol{h}_{l,e}^H \in \mathbb{C}^{1\times N}$ denotes the channel matrix of the l-th RIS to the eavesdropper link. Like most papers [13]–[23] on PLS performance enhancement assisted by RIS, we assume that BSs can obtain the required CSI. CSI acquisition can be completed based on channel estimation, which has gained extensive attention on RIS-assisted systems [29]–[32]. The rationale for assuming that the eavesdropper's CSI is known can be understood from two perspectives. First, if the eavesdropper is an active user within the system but is not trusted by the legitimate receiver [13], it is reasonable to assume that the eavesdropper's CSI is accessible. Second, assuming perfect knowledge of the CSI can be viewed as an upper-bound solution for the system, providing a useful benchmark to guide system design when the eavesdropper's CSI is only partially known [17].

In downlink transmissions, we assume that orthogonal frequency bands are adopted for adjacent BSs to eliminate inter-cell interference [25]. We only concentrate on each RIS assisting its nearest BS. On one hand, recent studies have shown that practical reflecting elements of RIS can only provide adjustable phase shifts for signals within a certain frequency band, while exhibiting nearly fixed phase shifts (0 or 2π) for signals in other frequency bands [33]. This characteristic indicates that RIS can serve at most one BS and its associated users for communication. On the other hand, due to the product path loss effect, we only consider the signals reflected by the RIS closest to the BS. Hence, the BS-RIS pair is fixed as

(s,l) in the latter analysis. For multiple users served by one BS, all downlink transmissions are carried out on the same frequency band, which means that users served by the same BS share the same spectrum resources. And each eavesdropper operates within the frequency band of the corresponding BS it is monitoring to capture the confidential signal. In the wiretap scenario, the s-th BS transmits confidential message $\boldsymbol{x}_{s,k} = \boldsymbol{\omega}_{s,k}c_k$ to user k, where $\boldsymbol{\omega}_{s,k} \in \mathbb{C}^{M\times 1}$ denotes TBF vector at the s-th BS and $c_k \sim \mathcal{CN}(0,1)$ is the confidential data towards user k. Since one BS may provide service for more than one legitimate user, we define set $\mathcal{U}(s)$ as legitimate users served by the s-th BS and $\boldsymbol{\omega}_{s,j} \in \mathbb{C}^{M\times 1}$ as the TBF vector from the s-th BS to the j-th user ($j \neq k, j \in \mathcal{U}(s)$) for all users served by the s-th BS. For simplicity, the TBF matrix at the s-th BS can be defined as $\boldsymbol{\Omega}_s = [\boldsymbol{\omega}_{s,1}, \boldsymbol{\omega}_{s,2}, \cdots, \boldsymbol{\omega}_{s,j}, \cdots, \boldsymbol{\omega}_{s,K}] \in \mathbb{C}^{M\times K}$. Hence, the confidential signal received by the k-th user served by the s-th BS can be modeled as

$$y_{s,k} = \underbrace{b_{s,k}\boldsymbol{h}_{s,k}^H\boldsymbol{\omega}_{s,k}c_k}_{\text{confidential signal}} + \sum_{j\neq k}^{\mathcal{U}(s)} \underbrace{b_{s,k}\boldsymbol{h}_{s,k}^H\boldsymbol{\omega}_{s,j}c_j}_{\text{intra-interference signal}} + \underbrace{n_u}_{\text{noise}}, \quad (5)$$

where $\mathbf{n}_u \sim \mathcal{CN}(0,\sigma_u^2)$ is the random additive white Gaussian noise (AWGN) of users. Further, the signal-to-interference-plus-noise ratio (SINR) expression for the k-th user served by the s-th BS can be represented as ($b_{s,k} = 1$ means the s-th BS serves the k-th user):

$$\gamma_{s,k} = \frac{|b_{s,k}\boldsymbol{h}_{s,k}^H\boldsymbol{\omega}_{s,k}|^2}{\sum_{j\neq k}^{\mathcal{U}(s)}|b_{s,k}\boldsymbol{h}_{s,k}^H\boldsymbol{\omega}_{s,j}|^2+\sigma_u^2}. \quad (6)$$

Then, the achievable rate of the k-th user served by the s-th BS can be written as

$$\begin{aligned} C_{s,k}(\boldsymbol{\omega}_{s,k},\boldsymbol{\Psi}_l,b_{s,k}) &= \log_2(1+\gamma_{s,k}) \\ &= \log_2(1+\frac{|b_{s,k}\boldsymbol{h}_{s,k}^H\boldsymbol{\omega}_{s,k}|^2}{\sum_{j\neq k}^{\mathcal{U}(s)}|b_{s,k}\boldsymbol{h}_{s,k}^H\boldsymbol{\omega}_{s,j}|^2+\sigma_u^2}). \end{aligned} \quad (7)$$

As for the eavesdropper around BS s, it attempts to eavesdrop on the confidential information sent by BS s to its served legitimate users. When the specific BS is allocated to serve the k-th user, the signal received by the eavesdropper wiretapping the k-th user served by the s-th BS can be denoted as

$$y_{s,e,k} = \underbrace{b_{s,k}\boldsymbol{h}_{s,e}^H\boldsymbol{\omega}_{s,k}c_k}_{\text{wiretapping signal}} + \sum_{j\neq k}^{\mathcal{U}(s)} \underbrace{b_{s,k}\boldsymbol{h}_{s,e}^H\boldsymbol{\omega}_{s,j}c_j}_{\text{intra-interference signal}} + \underbrace{n_e}_{\text{noise}}, \quad (8)$$

where $\mathbf{n}_e \sim \mathcal{CN}(0,\sigma_e^2)$ is the random AWGN of the eavesdropper. The SINR for the eavesdropper while wiretapping the k-th user served by the s-th BS can be expressed as

$$\gamma_{s,e,k} = \frac{|b_{s,k}\boldsymbol{h}_{s,e}^H\boldsymbol{\omega}_{s,k}|^2}{\sum_{j\neq k}^{\mathcal{U}(s)}|b_{s,k}\boldsymbol{h}_{s,e}^H\boldsymbol{\omega}_{s,j}|^2+\sigma_e^2}. \quad (9)$$

And the achievable wiretapping rate of the k-th user is described as

$$\begin{aligned} C_{s,e,k}(\boldsymbol{\omega}_{s,k},\boldsymbol{\Psi}_l,b_{s,k}) &= \log_2(1+\gamma_{s,e,k}) \\ &= \log_2(1+\frac{|b_{s,k}\boldsymbol{h}_{s,e}^H\boldsymbol{\omega}_{s,k}|^2}{\sum_{j\neq k}^{\mathcal{U}(s)}|b_{s,k}\boldsymbol{h}_{s,e}^H\boldsymbol{\omega}_{s,j}|^2+\sigma_e^2}). \end{aligned} \quad (10)$$

Thus, the SR which is used to characterize the PLS performance of the system for the k-th user served by BS s can be expressed as

$$C_{sec,k} = [C_{s,k}(\boldsymbol{\omega}_{s,k},\boldsymbol{\Psi}_l,b_{s,k}) - C_{s,e,k}(\boldsymbol{\omega}_{s,k},\boldsymbol{\Psi}_l,b_{s,k})]^+, \quad (11)$$

where $[*]^+ \triangleq \max[*,0]$ and $C_{sec,k} > 0$ means the secure communication for the k-th user. We can omit the non-negative operator since the optimal value of SR must be non-negative to prevent the confidential signal from being wiretapped [13].

C. Problem formulation

We have analyzed the SR expression for the k-th user in the previous subsection. There are total K legitimate users in the system, the whole SR can be written as

$$\begin{aligned} &\sum_{s\in\mathcal{S}}\sum_{k\in\mathcal{K}} C_{sec,k}(\boldsymbol{\omega}_{s,k},\boldsymbol{\Psi}_l,b_{s,k}) \\ &= \sum_{s\in\mathcal{S}}\sum_{k\in\mathcal{K}} [C_{s,k}(\boldsymbol{\omega}_{s,k},\boldsymbol{\Psi}_l,b_{s,k}) - C_{s,e,k}(\boldsymbol{\omega}_{s,k},\boldsymbol{\Psi}_l,b_{s,k})]^+, \end{aligned} \quad (12)$$

where $C_{s,k}(\boldsymbol{\omega}_{s,k},\boldsymbol{\Psi}_l,b_{s,k})$ and $C_{s,e,k}(\boldsymbol{\omega}_{s,k},\boldsymbol{\Psi}_l,b_{s,k})$ are given by (7) and (10), respectively. Since we intend to design secure TBF of BSs and configure phase shifts of RISs to suppress the signal leakage caused by malicious eavesdroppers as much as possible, the proposed SSRM-SUA problem can be formulated as

$$\max_{\boldsymbol{\Omega}_s,\boldsymbol{\Psi}_l,\mathcal{B}} \sum_{s\in\mathcal{S}}\sum_{k\in\mathcal{K}} C_{sec,k}(\boldsymbol{\omega}_{s,k},\boldsymbol{\Psi}_l,b_{s,k}) \quad (13a)$$

$$s.t. \quad b_{s,k} = \{0,1\}, \forall k \in \mathcal{K}, \forall s \in \mathcal{S}, \quad (13b)$$

$$\|\boldsymbol{b_k}\|_0 = 1, \forall k \in \mathcal{K}, \quad (13c)$$

$$\left\|\widetilde{\boldsymbol{b}}_{\boldsymbol{s}}\right\|_0 \geq 1, \forall s \in \mathcal{S}, \quad (13d)$$

$$\sum_{s\in\mathcal{S}} ||\boldsymbol{\Omega}_s||_F^2 \leq P_T, \forall s \in \mathcal{S}, \quad (13e)$$

$$\theta_{l,n} \in \mathcal{F}, \forall l \in \mathcal{L}, \forall n = 1,2,\cdots,N, \quad (13f)$$

where (13b), (13c) and (13d) are BSs-users association constraints. (13b) indicates the association status between the s-th BS and the k-th user, which takes values of 0 or 1. (13c) means the k-th user can only be served by one BS and (13d) denotes the s-th BS can serve more than one user. (13e) is the total maximum transmit power constraint for all BSs and (13f) is the discrete phase shifts constraint of L RISs. The proposed problem is hard to solve directly due to the non-convexity of the objective function and constraints. Meanwhile, the coupling relationship between variables $\boldsymbol{\Omega}_s$, $\boldsymbol{\Psi}_l$ and $\mathcal{B}$ makes the problem more complex to solve. In the following section, we will attempt to solve it efficiently.

III. Problem Analysis and Solution

In this section, we aim to solve the proposed SSRM-SUA problem (13). Since (13) is non-convex and hard to obtain the optimal solution, the AO method is adopted to tackle the intractable coupling relationship between variables $\boldsymbol{\Omega}_s$, $\boldsymbol{\Psi}_l$ and $\mathcal{B}$. Specifically, we divide the original problem (13) into three subproblems: i) secure TBF matrix $\boldsymbol{\Omega}_s$ optimization at BSs

with given $\mathbf{\Psi}_l$ and $\mathcal{B}$, ii) secure PBF matrix (RIS discrete phase shifts) $\mathbf{\Psi}_l$ optimization at RISs with given $\mathbf{\Omega}_s$ and $\mathcal{B}$, iii) secure BSs-users association matrix $\mathcal{B}$ optimization with given $\mathbf{\Omega}_s$ and $\mathbf{\Psi}_l$. We then optimize them alternately until a feasible solution is obtained.

A. Optimizing secure TBF matrix $\mathbf{\Omega}_s$

In this subsection, we focus on optimizing secure TBF matrix $\mathbf{\Omega}_s$ with given RIS phase shifts $\mathbf{\Psi}_l$ and secure BSs-users association matrix $\mathcal{B}$. Then we can drop constraints (13b), (13c), (13d) and (13f), respectively. Once the association matrix $\mathcal{B}$ is configured, BS allocated to the k-th user can be obtained. Hence, we only need to design TBF at the s-th BS for users served by it, which is defined as $\mathcal{U}(s)$. Then problem (13) can be further represented as

$$\max_{\mathbf{\Omega}_s} \sum_{s\in\mathcal{S}}\sum_{k\in\mathcal{U}(s)} [\log_2(1+\frac{|\mathbf{h}_{s,k}^H\boldsymbol{\omega}_{s,k}|^2}{\sum_{j\neq k}^{\mathcal{U}(s)}|\mathbf{h}_{s,k}^H\boldsymbol{\omega}_{s,j}|^2+\sigma_u^2}) - \log_2(1+\frac{|\mathbf{h}_{s,e}^H\boldsymbol{\omega}_{s,k}|^2}{\sum_{j\neq k}^{\mathcal{U}(s)}|\mathbf{h}_{s,e}^H\boldsymbol{\omega}_{s,j}|^2+\sigma_e^2})] \quad (14a)$$

$$s.t. \quad \sum_{s\in\mathcal{S}}||\mathbf{\Omega}_s||_F^2 \le P_T, \forall s\in\mathcal{S}, \forall k\in\mathcal{U}(s). \quad (14b)$$

To efficiently solve this subproblem, we need to transform it into tractable expression first. Since orthogonal frequency bands are adopted for adjacent BSs, TBF matrix for the s-th BS does not effect other BSs when BSs-users association matrix is given. Hence, we can focus on designing TBF matrix for the s-th BS in order until total S BSs. Define $\mathbf{W}_{s,k} = \boldsymbol{\omega}_{s,k}\boldsymbol{\omega}_{s,k}^H \in \mathbb{C}^{M\times M}$ and $\mathbf{W}_s = [\mathbf{W}_{s,1}, \mathbf{W}_{s,2}, \cdots, \mathbf{W}_{s,k}], \forall s\in\mathcal{S}, \forall k\in\mathcal{U}(s)$, then the actual achievable SR for the k-th user served by the s-th BS can be written as

$$\begin{aligned} C_{sec,k} &= \log_2(1+\frac{\mathrm{Tr}(\mathbf{W}_{s,k}\mathbf{h}_{s,k}\mathbf{h}_{s,k}^H)}{\sum_{j\neq k}^{\mathcal{U}(s)}\mathrm{Tr}(\mathbf{W}_{s,j}\mathbf{h}_{s,k}\mathbf{h}_{s,k}^H)+\sigma_u^2}) - \log_2(1+\frac{\mathrm{Tr}(\mathbf{W}_{s,k}\mathbf{h}_{s,e}\mathbf{h}_{s,e}^H)}{\sum_{j\neq k}^{\mathcal{U}(s)}\mathrm{Tr}(\mathbf{W}_{s,j}\mathbf{h}_{s,e}\mathbf{h}_{s,e}^H)+\sigma_e^2}) \\ &= \log_2\frac{\sum_{j\in\mathcal{U}(s)}\mathrm{Tr}(\mathbf{W}_{s,j}\mathbf{h}_{s,k}\boldsymbol{h}_{s,k}^H)+\sigma_u^2}{\sum_{j\neq k}^{\mathcal{U}(s)}\mathrm{Tr}(\mathbf{W}_{s,j}\mathbf{h}_{s,k}\mathbf{h}_{s,k}^H)+\sigma_u^2} \cdot \frac{\sum_{j\neq k}^{\mathcal{U}(s)}\mathrm{Tr}(\mathbf{W}_{s,j}\mathbf{h}_{s,e}\mathbf{h}_{s,e}^H)+\sigma_e^2}{\sum_{j\in\mathcal{U}(s)}\mathrm{Tr}(\mathbf{W}_{s,j}\mathbf{h}_{s,e}\mathbf{h}_{s,e}^H)+\sigma_e^2} \\ &= C_{1,k}(\mathbf{W}_s)+C_{2,k}(\mathbf{W}_s)+C_{3,k}(\mathbf{W}_s)+C_{4,k}(\mathbf{W}_s), \end{aligned} \quad (15)$$

where $C_{i,k}(\mathbf{W}_s)(i\in\{1,2,3,4\})$ are respectively given by

$$C_{1,k}(\mathbf{W}_s) = \log_2[\sum_{j\in\mathcal{U}(s)}\mathrm{Tr}(\mathbf{W}_{s,j}\mathbf{h}_{s,k}\mathbf{h}_{s,k}^H)+\sigma_u^2], \quad (16)$$

$$C_{2,k}(\mathbf{W}_s) = \log_2[\sum_{j\neq k}^{\mathcal{U}(s)}\mathrm{Tr}(\mathbf{W}_{s,j}\mathbf{h}_{s,e}\mathbf{h}_{s,e}^H)+\sigma_e^2], \quad (17)$$

$$C_{3,k}(\mathbf{W}_s) = -\log_2[\sum_{j\neq k}^{\mathcal{U}(s)}\mathrm{Tr}(\mathbf{W}_{s,j}\mathbf{h}_{s,k}\mathbf{h}_{s,k}^H)+\sigma_u^2], \quad (18)$$

$$C_{4,k}(\mathbf{W}_s) = -\log_2[\sum_{j\in\mathcal{U}(s)}\mathrm{Tr}(\mathbf{W}_{s,j}\mathbf{h}_{s,e}\mathbf{h}_{s,e}^H)+\sigma_e^2]. \quad (19)$$

We can observe that the objective function (15) is still non-convex since there exists the difference form of convex function (DC) [34], which is hard to solve. To derive the lower bound for (15), we adopt SCA method [35], [36] to handle non-concave $C_{3,k}(\mathbf{W}_s)$ and $C_{4,k}(\mathbf{W}_s)$. Specifically, the following proposition is applied to linearize the non-concave parts [37], [38].

***Proposition* 1:** If x is a positive scalar and $f(x) = -\frac{xy}{\ln 2} + \log_2 x + \frac{1}{\ln 2}$, then we can have

$$-\log_2 y = \max_{x>0} f(x) \quad (20)$$

and the optimal solution to the right-hand side of (20) is $x = \frac{1}{y}$.

Proof: The proof can be finished by setting $\frac{\partial f(x)}{\partial x} = 0$ since $f(x)$ is concave. ■

According to ***Proposition 1***, in the t-th iteration, we can obtain the lower bound of $C_{3,k}(\mathbf{W}_s)$ around the given TBF point $\mathbf{W}_s^{(t-1)}$ acquired in the $(t-1)$-th iteration as the following:

$$\begin{aligned} C_{3,k}(\mathbf{W}_s) &= -\log_2[\sum_{j\neq k}^{\mathcal{U}(s)}\mathrm{Tr}(\mathbf{W}_{s,j}\mathbf{h}_{s,k}\mathbf{h}_{s,k}^H)+\sigma_u^2] \\ &\ge C_{3,k}^{(t)}\left(\mathbf{W}_s^{(t)}, \mathbf{W}_s^{(t-1)}\right) = \max_{x_{3,k}^{(t)}>0}\log_2 x_{3,k}^{(t)} + \frac{1}{\ln 2} \\ &\quad - \frac{x_{3,k}^{(t)}\left(\sum_{j\neq k}^{\mathcal{U}(s)}\mathrm{Tr}(\mathbf{W}_{s,j}^{(t)}\mathbf{h}_{s,k}\mathbf{h}_{s,k}^H)+\sigma_u^2\right)}{\ln 2}, \end{aligned} \quad (21)$$

where the closed-form of $x_{3,k}^{(t)}$ is given by

$$x_{3,k}^{(t)} = \left(\sum_{j\neq k}^{\mathcal{U}(s)}\mathrm{Tr}(\mathbf{W}_{s,j}^{(t-1)}\mathbf{h}_{s,k}\mathbf{h}_{s,k}^H)+\sigma_u^2\right)^{-1}. \quad (22)$$

Likewise, we can also obtain the lower bound of $C_{4,k}(\mathbf{W})$ in the t-th iteration:

$$\begin{aligned} C_{4,k}(\mathbf{W}_s) &= -\log_2[\sum_{j\in\mathcal{U}(s)}\mathrm{Tr}(\mathbf{W}_{s,j}\mathbf{h}_{s,e}\mathbf{h}_{s,e}^H)+\sigma_e^2] \\ &\ge C_{4,k}^{(t)}\left(\mathbf{W}_s^{(t)}, \mathbf{W}_s^{(t-1)}\right) = \max_{x_{4,k}^{(t)}>0}\log_2 x_{4,k}^{(t)} + \frac{1}{\ln 2} \\ &\quad - \frac{x_{4,k}^{(t)}\left(\sum_{j\in\mathcal{U}(s)}\mathrm{Tr}(\mathbf{W}_{s,j}^{(t)}\mathbf{h}_{s,e}\mathbf{h}_{s,e}^H)+\sigma_e^2\right)}{\ln 2}, \end{aligned} \quad (23)$$

where the closed-form of $x_{4,k}^{(t)}$ is given by

$$x_{4,k}^{(t)} = \left(\sum_{j\in\mathcal{U}(s)}\mathrm{Tr}(\mathbf{W}_{s,j}^{(t-1)}\mathbf{h}_{s,e}\mathbf{h}_{s,e}^H)+\sigma_e^2\right)^{-1}. \quad (24)$$

After successfully obtaining the lower bound expressions $C_{3,k}^{(t)}\left(\mathbf{W}_s^{(t)}, \mathbf{W}_s^{(t-1)}\right)$ and $C_{4,k}^{(t)}\left(\mathbf{W}_s^{(t)}, \mathbf{W}_s^{(t-1)}\right)$ in the t-th iteration, the convex lower bound of SR for the k-th user served by the s-th BS, namely (15), can be approximated as

$$\begin{aligned} &C_{sec,k}^{(t)}(\mathbf{W}_s^{(t)}) \ge C_{sec,k}^{(t)}(\mathbf{W}_s^{(t)}, \mathbf{W}_s^{(t-1)}) \\ &= C_{1,k}^{(t)}(\mathbf{W}_s^{(t)}) + C_{2,k}^{(t)}(\mathbf{W}_s^{(t)}) \\ &+ C_{3,k}^{(t)}(\mathbf{W}_s^{(t)}, \mathbf{W}_s^{(t-1)}) + C_{4,k}^{(t)}(\mathbf{W}_s^{(t)}, \mathbf{W}_s^{(t-1)}). \end{aligned} \quad (25)$$

Therefore, for the s-th BS, the TBF design problem in the t-th iteration can be reformulated as

$$\max_{\mathbf{W}_s^{(t)}} \sum_{k\in\mathcal{U}(s)} C_{sec,k}^{(t)}(\mathbf{W}_s^{(t)}, \mathbf{W}_s^{(t-1)}) \tag{26a}$$

$$s.t.\ \ \mathrm{Tr}(\mathbf{W}_{s,k}^{(t)}) \le P_s, \forall s\in\mathcal{S}, \forall k\in\mathcal{U}(s), \tag{26b}$$

$$\mathbf{W}_{s,k}^{(t)} \succeq \mathbf{0}, \forall s\in\mathcal{S}, \forall k\in\mathcal{U}(s), \tag{26c}$$

$$\mathrm{rank}(\mathbf{W}_{s,k}^{(t)}) = 1, \forall s\in\mathcal{S}, \forall k\in\mathcal{U}(s), \tag{26d}$$

where (26c) and (26d) are constraints introduced to guarantee $\mathbf{W}_{s,k}^{(t)} = \boldsymbol{\omega}_{s,k}^{(t)}\boldsymbol{\omega}_{s,k}^{H\ (t)}$. We drop constraint (26d) since it is non-convex by adopting SDR method. Then problem (26) can be efficiently solved by convex solver such as mosek. After obtaining $\mathbf{W}_{s,k}^{(t)}$, we have the following proposition:

***Proposition* 2:** The optimal solution $\mathbf{W}_{s,k}^{(t)}$ to problem (26) relaxing the constraint (26d) is always rank-one.

Proof: Please refer to Appendix I. ∎

With the obtained rank-one solution, the feasible optimal solution $\boldsymbol{\omega}_{s,k}^{(t)}$ can be further recovered by performing eigenvalue decomposition and the TBF matrix for BS s in the t-th iteration can be acquired by

$$\boldsymbol{\Omega}_s^{(t)} = [\boldsymbol{\omega}_{s,1}^{(t)}, \cdots, \boldsymbol{\omega}_{s,j}^{(t)}, \cdots, \boldsymbol{\omega}_{s,k}^{(t)}], \forall s\in\mathcal{S}, \forall k\in\mathcal{U}(s). \tag{27}$$

B. Optimizing secure PBF matrix $\boldsymbol{\Psi}_l$ of RISs

In this subsection, we intend to optimize secure PBF matrix $\boldsymbol{\Psi}_l$ of RISs deployed around BSs with given secure TBF matrix $\boldsymbol{\Omega}_s$ and secure BSs-users association matrix $\mathcal{B}$. We can drop constraints (13b), (13c), (13d) and (13e), respectively. Once the secure association matrix is obtained, BSs serving each user can be determined. As mentioned earlier, users served by the k-th BS is defined as set $\mathcal{U}(s)$. Then problem (13) can be reformulated as

$$\max_{\boldsymbol{\Psi}_l} \sum_{s\in\mathcal{S}}\sum_{k\in\mathcal{U}(s)} [\log_2(1+\frac{|\mathbf{h}_{s,k}^H\boldsymbol{\omega}_{s,k}|^2}{\sum_{j\neq k}^{\mathcal{U}(s)}|\mathbf{h}_{s,k}^H\boldsymbol{\omega}_{s,j}|^2+\sigma_u^2}) - \log_2(1+\frac{|\mathbf{h}_{s,e}^H\boldsymbol{\omega}_{s,k}|^2}{\sum_{j\neq k}^{\mathcal{U}(s)}|\mathbf{h}_{s,e}^H\boldsymbol{\omega}_{s,j}|^2+\sigma_e^2})] \tag{28a}$$

$$s.t.\ \ \theta_{l,n}\in\mathcal{F}, \forall l\in\mathcal{L}, \forall n=1,2,\cdots,N. \tag{28b}$$

Due to the existence of non-convex constraint (28b) and non-convex objective function, problem (28) is hard to solve. Similar to the optimization of TBF vector, we can still optimize the l-th RIS deployed to assist the s-th BS ($l=s$) in order until total L RISs. For the l-th RIS around the s-th BS, we define $\mathbf{v}_l = [e^{j\theta_{l,1}}, e^{j\theta_{l,2}}, \cdots, e^{j\theta_{l,N}}]^H \in \mathbb{C}^{N\times 1}$ as the equivalent phase shifts vector of the l-th RIS and then constraint (28b) is actually equivalent to unit modulus constraint $|\mathbf{v}_{l,n}| = 1, \forall l\in\mathcal{L}, \forall n$. Then we can rewrite $\mathbf{h}_{s,k}^H = \mathbf{h}_{d,s,k}^H + \mathbf{h}_{l,k}^H\boldsymbol{\Psi}_l\mathbf{G}_{s,l}$ as $\mathbf{h}_{s,k}^H = \mathbf{h}_{d,s,k}^H + \mathbf{v}_l^H\mathbf{H}_{s,k}$, where $\mathbf{H}_{s,k} = \mathrm{diag}(\mathbf{h}_{l,k}^H)\mathbf{G}_{s,l} \in \mathbb{C}^{N\times M}$. Further, we define $\widetilde{\mathbf{v}}_l = [\mathbf{v}_l, 1] \in \mathbb{C}^{(N+1)\times 1}$ and $\widetilde{\mathbf{H}}_{s,k} = \begin{bmatrix}\mathbf{H}_{s,k}\\ \mathbf{h}_{d,s,k}^H\end{bmatrix}$, then we can transform $|\mathbf{h}_{s,k}^H\boldsymbol{\omega}_{s,k}|^2$ into

$$|\mathbf{h}_{s,k}^H\boldsymbol{\omega}_{s,k}|^2 = |\widetilde{\mathbf{v}}_l^H\widetilde{\mathbf{H}}_{s,k}\boldsymbol{\omega}_{s,k}|^2. \tag{29}$$

As for the eavesdropper around BS s, we also define $\mathbf{H}_{s,e} = \mathrm{diag}(\mathbf{h}_{l,e}^H)\mathbf{G}_{s,l}$ and $\widetilde{\mathbf{H}}_{s,e,k} = \begin{bmatrix}\mathbf{H}_{s,e}\\ \mathbf{h}_{de,s}^H\end{bmatrix}$, Then $|\mathbf{h}_{s,e}^H\boldsymbol{\omega}_{s,k}|^2$ can be written as

$$|\mathbf{h}_{s,e}^H\boldsymbol{\omega}_{s,k}|^2 = |\widetilde{\mathbf{v}}_l^H\widetilde{\mathbf{H}}_{s,e,k}\boldsymbol{\omega}_{s,k}|^2. \tag{30}$$

As a consequence, the achievable SR for the k-th user can be expressed as

$$\begin{aligned} C_{sec,k} &= \log_2(1+\frac{|\widetilde{\mathbf{v}}_l^H\widetilde{\mathbf{H}}_{s,k}\boldsymbol{\omega}_{s,k}|^2}{\sum_{j\neq k}^{\mathcal{U}(s)}|\widetilde{\mathbf{v}}_l^H\widetilde{\mathbf{H}}_{s,k}\boldsymbol{\omega}_{s,j}|^2+\sigma_u^2}) - \log_2(1+\frac{|\widetilde{\mathbf{v}}_l^H\widetilde{\mathbf{H}}_{s,e,k}\boldsymbol{\omega}_{s,k}|^2}{\sum_{j\neq k}^{\mathcal{U}(s)}|\widetilde{\mathbf{v}}_l^H\widetilde{\mathbf{H}}_{s,e,k}\boldsymbol{\omega}_{s,j}|^2+\sigma_e^2}) \\ &= \log_2(1+\frac{|\widetilde{\mathbf{v}}_l^H\bar{\mathbf{H}}_{s,k}\boldsymbol{\omega}_{s,k}|^2}{\sum_{j\neq k}^{\mathcal{U}(s)}|\widetilde{\mathbf{v}}_l^H\bar{\mathbf{H}}_{s,k}\boldsymbol{\omega}_{s,j}|^2+1}) - \log_2(1+\frac{|\widetilde{\mathbf{v}}_l^H\bar{\mathbf{H}}_{s,e,k}\boldsymbol{\omega}_{s,k}|^2}{\sum_{j\neq k}^{\mathcal{U}(s)}|\widetilde{\mathbf{v}}_l^H\bar{\mathbf{H}}_{s,e,k}\boldsymbol{\omega}_{s,j}|^2+1}) \\ &= F_{1,k}(\widetilde{\mathbf{v}}_l) + F_{2,k}(\widetilde{\mathbf{v}}_l) + F_{3,k}(\widetilde{\mathbf{v}}_l), \end{aligned} \tag{31}$$

where normalization terms $\bar{\mathbf{H}}_{s,k} = \widetilde{\mathbf{H}}_{s,k}\sigma_u^{-1}$ and $\bar{\mathbf{H}}_{s,e,k} = \widetilde{\mathbf{H}}_{s,e,k}\sigma_e^{-1}$. Specifically, $F_{i,k}(\widetilde{\mathbf{v}}_l)$ $(i\in\{1,2,3\})$ are respectively given by

$$F_{1,k}(\widetilde{\mathbf{v}}_l) = \log_2(1+\frac{|\widetilde{\mathbf{v}}_l^H\bar{\mathbf{H}}_{s,k}\boldsymbol{\omega}_{s,k}|^2}{\sum_{j\neq k}^{\mathcal{U}(s)}|\widetilde{\mathbf{v}}_l^H\bar{\mathbf{H}}_{s,k}\boldsymbol{\omega}_{s,j}|^2+1}), \tag{32}$$

$$F_{2,k}(\widetilde{\mathbf{v}}_l) = \log_2(1+\sum_{j\neq k}^{\mathcal{U}(s)}|\widetilde{\mathbf{v}}_l^H\bar{\mathbf{H}}_{s,e,k}\boldsymbol{\omega}_{s,j}|^2), \tag{33}$$

$$F_{3,k}(\widetilde{\mathbf{v}}_l) = -\log_2(1+\sum_{j=1}^{\mathcal{U}(s)}|\widetilde{\mathbf{v}}_l^H\bar{\mathbf{H}}_{s,e,k}\boldsymbol{\omega}_{s,j}|^2). \tag{34}$$

Due to the existence of DC form in objective function (31), the non-convex optimization problem can not be solved directly. To transform it into a more tractable form, we first introduce the following proposition [39], [40].

***Proposition* 3:** For the given point $(x^{(t)}, y^{(t)})$, we have the following inequality

$$\ln(1+\frac{|x|^2}{y}) \ge \ln(1+\frac{|x^{(t)}|^2}{y^{(t)}}) - \frac{|x^{(t)}|^2}{y^{(t)}} + \frac{2\Re\{x^{(t)*}x\}}{y^{(t)}} - \frac{|x^{(t)}|^2(x^2+y)}{y^{(t)}(|x^{(t)}|^2+y^{(t)})} \tag{35}$$

According to ***Proposition 3***, we can directly obtain the lower bound of $F_{1,k}(\widetilde{\mathbf{v}}_l)$ in the t-th iteration as $\widetilde{F}_{1,k}(\widetilde{\mathbf{v}}_l)$

$$\widetilde{F}_{1,k}(\widetilde{\mathbf{v}}_l) = \frac{1}{\ln 2}[G_0^{(t)}2\Re\{\boldsymbol{\omega}_{s,k}^{(t)H}\bar{\mathbf{H}}_{s,k}^H\widetilde{\mathbf{v}}_l^{(t-1)}\widetilde{\mathbf{v}}_l^{(t)H}\bar{\mathbf{H}}_{s,k}\boldsymbol{\omega}_{s,k}^{(t)}\} - G_1^{(t)}(1+\sum_{j=1}^{\mathcal{U}(s)}|\widetilde{\mathbf{v}}_l^{(t)H}\bar{\mathbf{H}}_{s,k}\boldsymbol{\omega}_{s,j}^{(t)}|^2)] + C_1, \tag{36}$$

where $G_0^{(t)}$ and $G_1^{(t)}$ are separately denoted by

$$G_0^{(t)} = (1+\sum_{j\neq k}^{\mathcal{U}(s)}|\widetilde{\mathbf{v}}_l^{(t-1)H}\bar{\mathbf{H}}_{s,k}\boldsymbol{\omega}_{s,j}^{(t)}|^2)^{-1}, \tag{37}$$

$$G_1^{(t)} = \frac{G_0^{(t)} |\widetilde{\mathbf{v}}_l^{(t-1)H} \bar{\mathbf{H}}_{s,k} \boldsymbol{\omega}_{s,k}^{(t)}|^2}{1 + \sum_{j=1}^{\mathcal{U}(s)} |\widetilde{\mathbf{v}}_l^{(t-1)H} \bar{\mathbf{H}}_{s,k} \boldsymbol{\omega}_{s,j}^{(t)}|^2}. \tag{38}$$

For $F_{2,k}(\widetilde{\mathbf{v}}_l)$, the lower bound $\widetilde{F}_{2,k}(\widetilde{\mathbf{v}}_l)$ can also be acquired by letting $y = 1$ in ***Proposition 3***

$$\begin{aligned}\widetilde{F}_{2,k}(\widetilde{\mathbf{v}}_l) = \frac{1}{\ln 2}[\sum_{j\neq k}^{\mathcal{U}(s)} 2\Re\{\boldsymbol{\omega}_{s,j}^{(t)^H} \bar{\mathbf{H}}_{s,e,k}^H \widetilde{\mathbf{v}}_l^{(t-1)} \widetilde{\mathbf{v}}_l^{(t)H} \bar{\mathbf{H}}_{s,e,k} \boldsymbol{\omega}_{s,j}^{(t)}\} \\ - G_2^{(t)}(1 + \sum_{j\neq k}^{\mathcal{U}(s)} |\widetilde{\mathbf{v}}_l^{(t)H} \bar{\mathbf{H}}_{s,e,k} \boldsymbol{\omega}_{s,j}^{(t)H}|^2)] + C_2,\end{aligned} \tag{39}$$

where $G_2^{(t)}$ is denoted by

$$G_2^{(t)} = \frac{\sum_{j\neq k}^{\mathcal{U}(s)} |\widetilde{\mathbf{v}}_l^{(t-1)H} \bar{\mathbf{H}}_{s,e,k} \boldsymbol{\omega}_{s,j}^{(t)}|^2}{1 + \sum_{j\neq k}^{\mathcal{U}(s)} |\widetilde{\mathbf{v}}_l^{(t-1)H} \bar{\mathbf{H}}_{s,e,k} \boldsymbol{\omega}_{s,j}^{(t)}|^2}. \tag{40}$$

And the lower bound of $F_{3,k}(\widetilde{\mathbf{v}}_l)$ can be obtained by utilizing the inequality $\ln(1+x) \leq \ln(1+x') + (x-x')/(1+x'), \forall x \geq 0, x' \geq 0$ at the given point x' [39], which is expressed by

$$\widetilde{F}_{3,k}(\widetilde{\mathbf{v}}_l) = -\frac{1}{\ln 2} G_3^{(t)} \sum_{j=1}^{\mathcal{U}(s)} |\widetilde{\mathbf{v}}_l^{(t)H} \bar{\mathbf{H}}_{s,e,k} \boldsymbol{\omega}_{s,j}^{(t)}|^2 + C_3, \tag{41}$$

where $G_3^{(t)}$ is denoted by

$$G_3^{(t)} = (1 + \sum_{j=1}^{\mathcal{U}(s)} |\widetilde{\mathbf{v}}_l^{(t-1)H} \bar{\mathbf{H}}_{s,e,k} \boldsymbol{\omega}_{s,j}^{(t)}|^2)^{-1}. \tag{42}$$

After respectively approximating $F_{1,k}(\widetilde{\mathbf{v}}_l)$, $F_{2,k}(\widetilde{\mathbf{v}}_l)$ and $F_{3,k}(\widetilde{\mathbf{v}}_l)$, the phase shifts design problem for the s-th BS served by the l-th RIS in the t-th iteration can be reformulated as the following

$$\max_{\widetilde{\mathbf{v}}_l^{(t)}} \quad \sum_{k\in\mathcal{U}(s)} \widetilde{F}_{1,k}(\widetilde{\mathbf{v}}_l) + \widetilde{F}_{2,k}(\widetilde{\mathbf{v}}_l) + \widetilde{F}_{3,k}(\widetilde{\mathbf{v}}_l) \tag{43a}$$

$$s.t. \quad |\mathbf{v}_{l,n}^{(t)}| = 1, \forall l \in \mathcal{L}, \forall n = 1, 2, \cdots, N+1. \tag{43b}$$

To tackle the RIS unit modulus constraint, we first transform the non-convex objective function into the quadratic form as

$$\max_{\widetilde{\mathbf{v}}_l^{(t)}} \quad -\widetilde{\mathbf{v}}_l^{(t)H} \mathbf{C} \widetilde{\mathbf{v}}_l^{(t)} + 2\Re\{\widetilde{\mathbf{v}}_l^{(t)H} \mathbf{D}\} + E \tag{44a}$$

$$s.t. \quad |\mathbf{v}_{l,n}^{(t)}| = 1, \forall l \in \mathcal{L}, \forall n = 1, 2, \cdots, N+1. \tag{44b}$$

where $\mathbf{C} = \sum_{k\in\mathcal{U}(s)} \mathbf{C}_k$ and $\mathbf{D} = \sum_{k\in\mathcal{U}(s)} \mathbf{D}_k$, which are respectively given by

$$\begin{aligned}\mathbf{C}_k = G_1^{(t)} \sum_{j=1}^{\mathcal{U}(s)} \bar{\mathbf{H}}_{s,k} \boldsymbol{\omega}_{s,j}^{(t)} \boldsymbol{\omega}_{s,j}^{(t)H} \bar{\mathbf{H}}_{s,k}^H \\ + G_2^{(t)} \sum_{j\neq k}^{\mathcal{U}(s)} \bar{\mathbf{H}}_{s,e,k} \boldsymbol{\omega}_{s,j}^{(t)} \boldsymbol{\omega}_{s,j}^{(t)H} \bar{\mathbf{H}}_{s,e,k}^H \\ + G_3^{(t)} \sum_{j=1}^{\mathcal{U}(s)} \bar{\mathbf{H}}_{s,e,k} \boldsymbol{\omega}_{s,j}^{(t)} \boldsymbol{\omega}_{s,j}^{(t)H} \bar{\mathbf{H}}_{s,e,k}^H,\end{aligned} \tag{45}$$

$$\begin{aligned}\mathbf{D}_k = G_0^{(t)} \bar{\mathbf{H}}_{s,k} \boldsymbol{\omega}_{s,k}^{(t)} \boldsymbol{\omega}_{s,k}^{(t)H} \bar{\mathbf{H}}_{s,k}^H \widetilde{\mathbf{v}}_l^{(t-1)} \\ + \sum_{j\neq k}^{\mathcal{U}(s)} \bar{\mathbf{H}}_{s,e,k} \boldsymbol{\omega}_{s,j}^{(t)} \boldsymbol{\omega}_{s,j}^{(t)H} \bar{\mathbf{H}}_{s,e,k}^H \widetilde{\mathbf{v}}_l^{(t-1)}.\end{aligned} \tag{46}$$

Besides, $E = C_1 + C_2 + C_3$ is the constant term.

To solve problem (44), inspired by [41], we iteratively optimize each reflecting element of $\widetilde{\mathbf{v}}_l^{(t)}$ while keeping the other N elements fixed. With $\mathbf{C}$ being a Hermitian matrix, we can derive

$$\begin{aligned}\widetilde{\mathbf{v}}_l^{(t)H} \mathbf{C} \widetilde{\mathbf{v}}_l^{(t)} = \widetilde{v}_{l,n}^* C_{n,n} \widetilde{v}_{l,n} + \sum_{i=1,i\neq n}^{N+1} \sum_{j=1,j\neq n}^{N+1} \widetilde{v}_{l,i}^* C_{i,j} \widetilde{v}_{l,j} \\ + 2\Re\{\sum_{j=1,j\neq n}^{N+1} \widetilde{v}_{l,n}^* C_{n,j} \widetilde{v}_{l,j}\},\end{aligned} \tag{47}$$

$$\widetilde{\mathbf{v}}_l^{(t)H} \mathbf{D} = \widetilde{v}_{l,n}^* D_n + \sum_{i=1,i\neq n}^{N+1} \widetilde{v}_{l,i}^* D_i, \tag{48}$$

where $\widetilde{v}_{l,n}$ is the n-th reflecting element of phase shifts vector $\widetilde{\mathbf{v}}_l^{(t)}$. $C_{i,j}$ denotes the element in the i-th row and j-th column of matrix $\mathbf{C}$, and D_i represents the i-th element of matrix $\mathbf{D}$. Combining (47) and (48) , we can rewrite problem (44) as

$$\max_{\angle\widetilde{v}_{l,n}} \quad -C_{n,n} + 2\Re\{\widetilde{v}_{l,n}^*(D_n - \sum_{i=1,i\neq n}^{N+1} C_{n,i} \widetilde{v}_{l,i})\} \tag{49a}$$

$$s.t. \quad \angle\widetilde{v}_{l,n} \in \mathcal{F} \triangleq \left\{0, \frac{2\pi}{2^b}, ..., \frac{2\pi * (2^b - 1)}{2^b}\right\}. \tag{49b}$$

where $\angle\widetilde{v}_{l,n}$ is the argument of $\widetilde{v}_{l,n}$, representing the phase shift of the n-th element of the l-th RIS. Further, we define $f_n = D_n - \sum_{i=1,i\neq n}^{N+1} C_{n,i} \widetilde{v}_{l,i}$ with $\angle f_n$ being the argument of f_n. The optimal phase shift $\angle\widetilde{v}_{l,n}$ can be expressed as

$$\angle\widetilde{v}_{l,n}^{opt} = \arg \min_{\angle\widetilde{v}_{l,n}\in\mathcal{F}} |\angle f_n - \angle\widetilde{v}_{l,n}|. \tag{50}$$

C. Optimizing secure BSs-users association matrix $\mathcal{B}$

In this subsection, we aim to optimize secure BSs-users association matrix $\mathcal{B}$ with given secure TBF matrix $\boldsymbol{\Omega}_s$ and secure PBF matrix $\boldsymbol{\Psi}_l$ of RISs. When RISs are configured, channels between BSs and users / eavesdroppers also change. Hence, it can provide more possibilities for the secure pairing selection between BSs and users.

For S BSs and K users in the system, we can define all possible BSs-users association as $\mathcal{A}$. Simultaneously, users served by the s-th BS is defined as $\mathcal{U}(s)$ and BS serving the k-th user is denoted as $\mathcal{Z}(k)$. Besides, $\mathcal{D}$ is a subset of $\mathcal{A}$. For each BS, there exists more than one pairing $(s,k) \in \mathcal{D}$. And for each user, there can be at most one pairing $(s,k) \in \mathcal{D}$. Then problem (13) can be reformulated as

$$\max_{\mathcal{B}} \quad \sum_{s\in\mathcal{S}} \sum_{k\in\mathcal{K}} b_{s,k} C_{sec,s,k} \tag{51a}$$

$$s.t. \quad b_{s,k} = \{0,1\}, \forall (s,k) \in \mathcal{A}, \tag{51b}$$

$$\sum_{s\in\mathcal{Z}(k)} b_{s,k} = 1, \forall k \in \mathcal{K}, \tag{51c}$$

$$\sum_{k\in\mathcal{U}(s)} b_{s,k} \geq 1, \forall s \in \mathcal{S}. \tag{51d}$$

which is essentially an asymmetric allocation problem between S BSs and K users. For the feasible solution $\mathcal{D}$, if $(s,k)\in\mathcal{D}$, then $b_{s,k}=1$ and the security profit brought by the pairing between the s-th BS and the k-th user is $C_{sec,s,k}$.

To solve this allocation problem efficiently, we propose the two-step secure BSs-users association algorithm based on network optimization method and auction theory [42], [43]. Considering practical implementation constraints, directly incorporating the interference term in the utility calculation of each BS-user pair leads to highly complex nested optimization, especially due to the coupling introduced by the denominator. To strike a balance between computational efficiency and solution quality, we adopt a simplified approximation when computing the security profit during the BS-user association phase, where the interference term is temporarily excluded similar to the approach in [43]. This approximation allows the auction-based matching to be performed in a tractable manner. Importantly, after the association is determined, the interference term is fully restored in the subsequent joint optimization of transmit beamforming and RIS configuration, and the actual system SSR is recalculated based on the complete model. Assume each BS is connected to a virtual node e and $b_{s,k}$ represents data flow between the s-th BS and the k-th user. Then problem (51) can be converted into a typical minimum-cost network flow problem [42], [43]:

$$\min_{\mathcal{B}} \sum_{s\in\mathcal{S}}\sum_{k\in\mathcal{K}} -b_{s,k}C_{sec,s,k} \tag{52a}$$

$$s.t. \sum_{s\in\mathcal{Z}(k)} b_{s,k}=1, \forall k\in\mathcal{K}, \forall (s,k)\in\mathcal{A}, \tag{52b}$$

$$\sum_{k\in\mathcal{U}(s)} b_{s,k}-b_{e,s}=1, \forall s\in\mathcal{S}, \tag{52c}$$

$$\sum_{s\in\mathcal{S}} b_{e,s}=S_e, \forall s\in\mathcal{S}, \tag{52d}$$

where constraint (52b), (52c) and (52d) are new BSs-users association constraints with node e. (52b) means the k-th user can only receive a unit of data flow. (52c) indicates the s-th BS supplies a single data flow externally. And (52d) represents node e is the source node, generating $S_e=K-S$ units of data flow. According to the duality theory [42], by introducing Lagrange multipliers λ_s, μ_k and ρ, the dual problem of (52) can be written as

$$\min_{\lambda_s,\mu_k,\rho} \rho S_e+\sum_{k\in\mathcal{K}}\mu_k+\sum_{s\in\mathcal{S}}\lambda_s \tag{53a}$$

$$s.t. \quad \rho\geq\lambda_s, \forall s\in\mathcal{S}, \tag{53b}$$

$$\lambda_s+\mu_k\geq C_{sec,s,k}, \forall (s,k)\in\mathcal{A}, \tag{53c}$$

where μ_k of constraint (52b) denotes the price of the k-th user, $-\lambda_s$ of constraint (52c) represents the price of the s-th BS and ρ of constraint (52d) is the price of the virtual node e.

D. On the price increment ξ in the auction

Building on the dual program in (53), we specify the price update granularity used by the auction and quantify its algorithmic and optimality implications. In particular, let $0<\xi<\frac{1}{S}$ denote the price increment in each bidding step. Intuitively, a smaller ξ yields finer price discrimination (and thus potentially more bidding rounds), while a larger ξ accelerates convergence but risks violating the sufficient conditions for exact optimality.

To tackle the dual problem (53) in an auction form, we adopt a pair of prices (λ,μ) for BSs and users, and use ξ as the minimum raise in bids. For a feasible BS–user association $\mathcal{D}$ of (51), if (λ,μ) satisfies the following ξ-complementary slackness conditions

$$\begin{aligned} &\lambda_s+\mu_k\geq[C_{sec,s,k}]-\xi, && \forall (s,k)\in\mathcal{A},\\ &\lambda_s+\mu_k=[C_{sec,s,k}], && \forall (s,k)\in\mathcal{D},\\ &\lambda_s=\max_{i\in\mathcal{S}}\lambda_i, && (s,k)\in\mathcal{D}, \end{aligned} \tag{54}$$

then the prices are consistent with the assignment $\mathcal{D}$ and the auction terminates.

***Proposition* 4:** Assume $0<\xi<\frac{1}{S}$ and that the utilities used in the auction are integer-valued. If there exists a feasible assignment $\mathcal{D}$ of (51) and dual variables (λ,μ) that satisfy the ξ-complementary slackness conditions in (54), then $\mathcal{D}$ is an optimal solution to (51).

Proof: By standard network optimization arguments for minimum-cost flows and the auction interpretation of the dual, the ξ-complementary slackness ensures primal feasibility and dual feasibility with zero duality gap when $\xi<\frac{1}{S}$ and integer utilities are used. This can be proven by contradiction based on network optimization theory, which follows from Proposition 7.7 in [42] and Proposition 1 in [43], and is not repeated here for brevity. ■

Since $C_{sec,s,k}$ is generally real-valued, we adopt a standard integerization step: choose a scaling factor $\eta>0$, form $\eta C_{sec,s,k}$, and use $[C_{sec,s,k}]\triangleq\text{round}(\eta C_{sec,s,k})$ in (54). Define $\widehat{C}_{sec,s,k}\triangleq[C_{sec,s,k}]/\eta$. Then

$$\left|\widehat{C}_{sec,s,k}-C_{sec,s,k}\right|\leq\frac{1}{2\eta}, \quad \forall (s,k).$$

Consequently, the aggregate deviation between the final assignment value computed by the auction and the true value under (51) is bounded by $\frac{|\mathcal{D}|}{2\eta}$, which can be made negligible by choosing η sufficiently large. In practice, the impact of this rounding on the solution to (51) can be ignored.

The quantified impact of ξ can be stated as follows:

- *Optimality:* When $\xi<\frac{1}{S}$ and integer utilities are used as above, Proposition 4 guarantees that the auction reaches an optimal assignment of (51).
- *Complexity:* The number of bidding rounds grows roughly on the order of $1/\xi$. Thus, smaller ξ improves price resolution but increases iterations; larger ξ reduces iterations but may forfeit the exact optimality guarantee if $\xi\geq\frac{1}{S}$.

E. Two-step secure association auction

Based on the two-step auction algorithm, we can obtain secure BSs-users association $\mathcal{D}$. During the first step of the auction process, we first complete the bidding process for BSs to users. Specifically, we need to auction one user for each BS in this step, which ensures each BS serves at least one user,

avoiding the scenario of BSs being idle. In the first step of the auction, we sequentially select the s-th BS that has not completed bidding for user. Then, for the s-th BS, we find the optimal user k_s who can provide the maximum security profit $\Gamma_s = \max_{k\in\mathcal{U}(s)} (C_{sec,s,k} - \mu_k)$ in set $\mathcal{U}(s)$. To bid for user k_s, BS s will provide its expected price p_{s,k_s} until each BS has completed bidding for its optimal user. From all the bids received for user k_s, we select the BS that offers the highest price and allocate user k_s to it, while updating the price λ_k for user k_s. We consider the first step of the auction process complete when each BS is associated with a user and satisfies the complementary slackness condition (54).

Algorithm 1: Two-step secure association auction

Initialization: Feasible secure association $\mathcal{D}$, BSs-users prices pairs (λ, μ), auction increment ξ, ρ based on the complementary slackness condition (54);
The first step auction (BSs bid for users):
repeat
  For unallocated BSs in $\mathcal{D}$, they bid for the optimal user $k_s = \arg\Gamma_s$ with the maximum security profit $\Gamma_s = \max_{k\in\mathcal{U}(s)} (C_{sec,s,k} - \mu_k)$ (The set of BSs bidding for user k is defined as $\mathcal{Y}(k)$);
  Find the second security profit for BS s: $\Gamma_s^{'} = \max_{k\in\mathcal{U}(s),k\neq k_s} (C_{sec,s,k} - \mu_k)$ (For $\mathcal{U}(s)$ containing only one user, $\Gamma_s^{'} = -\inf$);
  BS s offers its own bid: $p_{s,k_s} = \mu_k + \Gamma_s + \xi - \Gamma_s^{'}$;
  User k obtains the highest bid received: $\mu_k = \max_{s\in\mathcal{Y}(k)} p_{s,k}$ and the bidding BS index is given by $s_k = \arg\mu_k$ (User k updates its price simultaneously);
  Update secure association $\mathcal{D}$ with (s_k, k), prices pairs (λ, μ) and virtual source node price $\rho = \max_{i\in\mathcal{S}} \lambda_i$;
until *all BSs have successfully auctioned users*;
The second step auction (users bid for BSs):
repeat
  For unallocated users in $\mathcal{D}$, they bid for the optimal BS $s_k = \arg\Gamma_k$ with the maximum security profit $\Gamma_k = \max_{s\in\mathcal{Z}(k)} (C_{sec,s,k} - \lambda_s)$;
  Find the second security profit for user k: $\Gamma_k^{'} = \max_{s\in\mathcal{Z}(k),s\neq s_k} (C_{sec,s,k} - \lambda_s)$ (For $\mathcal{Z}(k)$ containing only one BS, $\Gamma_k^{'} = -\inf$);
  Calculate $\zeta = \min(\rho - \lambda_{s_k}, \Gamma_k + \xi - \Gamma_k^{'})$, update $\lambda_{s_k} = \lambda_{s_k} + \zeta$, $\mu_k = \Gamma_k - \zeta$;
  Update secure association $\mathcal{D}$ with (s_k, k);
until *all remaining users have successfully auctioned*;
Output: Optimal secure association $\mathcal{B} = \mathcal{D}^*$.

Then, we can proceed to the second step of the auction process. In the first step of the auction, we have already auctioned one user for each BS. For the remaining users who have not been auctioned, they must be associated with BSs, which will be completed in the second step of the auction. Similar to the first step of the auction process, the second step of the auction is carried out from the perspective of users. We first sequentially select the user k who have not been auctioned. Among $\mathcal{Z}(k)$, we find the BS s_k that can provide the maximum security profit $\Gamma_k = \max_{s\in\mathcal{Z}(k)} (C_{sec,s,k} - \lambda_s)$. In order to be successfully auctioned by BS s_k, user k reduces its own price μ_k. We update the security profit of BS s_k and the price of user k in sequence, completing the second step of the auction. We summarize the two-step auction algorithm in **Algorithm 1**.

F. Overall optimization algorithm

We have analyzed the optimization of secure TBF matrix $\mathbf{\Omega}_s$, secure PBF matrix of RISs $\mathbf{\Psi}_l$ and secure BSs-users association matrix $\mathcal{B}$, respectively. In the entire optimization process, we alternately optimize variables $\mathbf{\Omega}_s$, $\mathbf{\Psi}_l$ and $\mathcal{B}$ until get the final stable SSR [1]. The overall alternating SSRM-SUA optimization algorithm is summarized in **Algorithm 2**. Now we check the convergence of it.

***Proposition* 5:** Let $R(\mathbf{\Omega}_s, \mathbf{\Psi}_l, \mathcal{B})$ denote the SSR objective of the main problem, and let $R^{(t)} \triangleq R\left(\mathbf{\Omega}_s^{(t)}, \mathbf{\Psi}_l^{(t)}, \mathcal{B}^{(t)}\right)$ be the value produced at iteration t. Assume that (i) in the TBF and RIS steps the algorithm maximizes (or, for the RIS QCQP with quantized phases, does not decrease) a *tight global lower-bounding* surrogate of R built at the previous iterate, and (ii) in the association step either the true association problem is solved exactly for the current $(\mathbf{\Omega}_s^{(t)}, \mathbf{\Psi}_l^{(t)})$ or a monotone acceptance rule is enforced (i.e., the candidate association is accepted only if it does not decrease R). Then $\{R^{(t)}\}$ is monotonically non-decreasing and, because the feasible set is compact (finite association choices, quantized RIS phases, and bounded transmit power), $\{R^{(t)}\}$ converges to a finite limit. Moreover, any accumulation point $(\mathbf{\Omega}_s^{\star}, \mathbf{\Psi}_l^{\star}, \mathcal{B}^{\star})$ is block-wise optimal in the sense that no single block update (TBF, RIS phases, or association) can further increase R given the other two blocks.

Proof: TBF step. With $\mathbf{\Psi}_l^{(t-1)}$ and $\mathcal{B}^{(t-1)}$ fixed, the constructed surrogate $\sum_{s,k} C_{\mathrm{sec},k}^{(t)}\left(\mathbf{W}_s; \mathbf{W}_s^{(t-1)}\right)$ is a *global lower bound* of the true objective and is *tight* at $\mathbf{W}_s^{(t-1)}$. Hence

$$\begin{aligned} R\left(\mathbf{\Omega}_s^{(t)}, \mathbf{\Psi}_l^{(t-1)}, \mathcal{B}^{(t-1)}\right) &\geq \sum_{s,k} C_{\mathrm{sec},k}^{(t)}\left(\mathbf{W}_s^{(t)}; \mathbf{W}_s^{(t-1)}\right) \\ &\geq \sum_{s,k} C_{\mathrm{sec},k}^{(t)}\left(\mathbf{W}_s^{(t-1)}; \mathbf{W}_s^{(t-1)}\right) \\ &= R\left(\mathbf{\Omega}_s^{(t-1)}, \mathbf{\Psi}_l^{(t-1)}, \mathcal{B}^{(t-1)}\right), \end{aligned}$$

so the true objective does not decrease.

RIS step. With $\mathbf{\Omega}_s^{(t)}$ and $\mathcal{B}^{(t-1)}$ fixed, the RIS update increases (or leaves unchanged) a tight global lower bound

[1]Consider the following scenario where the BS-user association (s, k) is not configured in a specific AO iteration, for BS-user pairs (s, k) that are currently not associated, we can generate a temporary beamforming vector assuming the association is active, which serves as a reasonable approximation for estimating SINR and secrecy rate. These vectors can be constructed using the secure beamforing strategy as in [13].

of R via coordinate-wise maximization over the quantized phases; thus the surrogate value is non-decreasing. Tightness at $\widetilde{\mathbf{v}}_l^{(t-1)}$ again yields

$$R\Big(\mathbf{\Omega}_s^{(t)}, \mathbf{\Psi}_l^{(t)}, \mathcal{B}^{(t-1)}\Big) \;\geq\; R\Big(\mathbf{\Omega}_s^{(t)}, \mathbf{\Psi}_l^{(t-1)}, \mathcal{B}^{(t-1)}\Big).$$

Association step. If the association problem is solved exactly for $(\mathbf{\Omega}_s^{(t)}, \mathbf{\Psi}_l^{(t)})$, the objective cannot decrease. If an auction-based candidate is used, the monotone acceptance test (accept only if the true R does not decrease) enforces

$$R\Big(\mathbf{\Omega}_s^{(t)}, \mathbf{\Psi}_l^{(t)}, \mathcal{B}^{(t)}\Big) \;\geq\; R\Big(\mathbf{\Omega}_s^{(t)}, \mathbf{\Psi}_l^{(t)}, \mathcal{B}^{(t-1)}\Big).$$

Combining the three blocks yields $R^{(t)} \geq R^{(t-1)}$. The feasible set is compact (power constraints and unit-modulus/quantized RIS phases bound the beamformed powers; the association set is finite), so $\{R^{(t)}\}$ converges. Finally, because each block is updated to a (coordinate-wise) maximizer of its tight surrogate and accepted only if it does not decrease the true objective, no single block change can improve R at a limit point, which gives the stated block-wise optimality. ■

Algorithm 2: Overall SSRM-SUA optimization algorithm

Initialization: Feasible solution $\mathbf{\Omega}_s^{(0)}$, $\mathbf{\Psi}_l^{(0)}$ and $\mathcal{B}^{(0)}$; The start iteration index $t = 1$, max iteration number T_{max} and convergence precision κ; Total transmit power P_T, BS transmit antennas M and RIS elements number N.

repeat

- Calculate system SSR $R^{(t-1)}$ with given $\mathbf{\Omega}_s^{(t-1)}$, $\mathbf{\Psi}_l^{(t-1)}$ and $\mathcal{B}^{(t-1)}$ by (12);
- Update $x_{3,k}^{(t)}$ and $x_{4,k}^{(t)}$ with given $\mathbf{\Omega}_s^{(t-1)}$, $\mathbf{\Psi}_l^{(t-1)}$ and $\mathcal{B}^{(t-1)}$ by (22) and (24);
- Solve problem (26) for S BSs with given $x_{3,k}^{(t)}$ and $x_{4,k}^{(t)}$, the optimal solution for BS s in the t-th iteration is $\mathbf{W}_s^{(t)}$. Then recover TBF matrix $\mathbf{\Omega}_s^{(t)}$ from $\mathbf{W}_s^{(t)}$.
- With given $\mathbf{\Omega}_s^{(t)}$, $\mathcal{B}^{(t-1)}$, solve problem (49) and obtain the optimal solution $\mathbf{v}_l^{(t)}$ for RIS l in the t-th iteration. Then $\mathbf{\Psi}_l^{(t)}$ is obtained.
- Update secure UA matrix $\mathcal{B}^{(t)}$ with $\mathbf{\Omega}_s^{(t)}$, $\mathbf{\Psi}_l^{(t)}$ by the two-step auction algorithm in **Algorithm 1**.
- Calculate system SSR $R^{(t)}$ with given $\mathbf{\Omega}_s^{(t)}$, $\mathbf{\Psi}_l^{(t)}$ and $\mathcal{B}^{(t)}$ by (12);
- Set $t = t + 1$;

until $|R^{(t)} - R^{(t-1)}| \leq \kappa$ *or reach* T_{max};

Output: The optimal solution $\mathbf{\Omega}_s^* = \mathbf{\Omega}_s^{(t)}$, $\mathbf{\Psi}_l^* = \mathbf{\Psi}_l^{(t)}$ and $\mathcal{B}^* = \mathcal{B}^{(t)}$.

The computational complexity of solving TBF optimization probelm (26) by cvx is given by $\mathcal{O}(M^{3.5}\log(\frac{1}{\kappa}))$. And the complexity of solving PBF optimization problem (49) lies in iteratively optimize each element of RIS with other elements fixed, namely $\mathcal{O}(N^2\log(\frac{1}{\kappa}))$. As for the secure BSs-users association optimization (53), the complexity mainly depends on the second step auction since $K > K - S$. The main calculation in auction process lies in bidding, which is given by $\mathcal{O}(\triangle SK)$ and $\triangle = \lceil(\max_{(s,k)\in\mathcal{A}} C_{sec,s,k} - \min_{(s,k)\in\mathcal{A}} C_{sec,s,k})/\xi\rceil$. Therefore, for total T iteration numbers, the computational complexity of **Algorithm 2** is $\mathcal{O}(T(SM^{3.5}\log(\frac{1}{\kappa}) + LN^2\log(\frac{1}{\kappa}) + \triangle SK))$.

IV. Numerical Simulations

A. Simulation Scenario

In this subsection, numerical simulations are conducted to evaluate the effectiveness of the proposed algorithm in enhancing system security. We simulate the wiretap scenario within a specified three-dimensional spatial region $\mathcal{R}$. Three BSs are deployed at (0m, -100m), (0m, 400m) and (400m, 400m), respectively. Meanwhile, three malicious eavesdroppers are respectively positioned at locations (100m, 0m), (100m, 300m) and (300m, 300m) to eavesdrop on the specific BS. Besides, K legitimate users are randomly generated within a region with a center at (200m, 200m) and a radius of 50m. The height ranges for BSs, users and the eavesdropper are (5m, 30m), (1m, 30m) and (1m, 30m) respectively. Simultaneously, we deploy a single RIS in a square area of 100 m^2 around each BS to assist its secure communication with legitimate users. The number of RISs deployed is the same as the number of BSs ($L = S$).

TABLE I
Simulation Parameters

Parameters	Values
Spatial simulation region $\mathcal{R}$ (m^3)	500× 500×30
Number of antennas at each BS (M)	4
Number of reflecting elements at each RIS (N)	16
Transmit power constraint at each BS (P_s)	1 W
RIS phase resolution (b)	3 bit
Noise power at users and eavesdroppers (σ_u^2)	-80dBm
Convergence precision (κ)	10^{-4}
Price increment in the auction (ξ)	0.2

We model the large-scale path loss as $p_l = p_{l,0}(\frac{d}{d_0})^{-\beta}$, where $p_{l,0}$ is the path loss for reference distance $d_0 = 1$m and β is the path loss exponent. The path loss exponents for each BS-RIS link, BS-user link, BS-Eav link, RIS-user link and RIS-Eav link are set as $\beta_{BR} = 2.2$, $\beta_{BU} = 3.5$, $\beta_{BE} = 3.5$, $\beta_{RU} = 2$ and $\beta_{RE} = 2$, respectively. We assume that each BS-user link and BS-Eav link follow Rayleigh fading, each BS-RIS link, RIS-user link and RIS-Eav link follow Rician fading. The specific simulation parameters are shown in Table I. Except for the parameters being analyzed, all other parameters are set to their default values.

B. Convergence Analysis

We check the convergence of the proposed **Algorithm 2**. As shown in Fig.2, we plot the convergence performance of the proposed algorithm under different number of RIS elements and legitimate users. It can be observed that the proposed algorithm converges to a stable value within a finite number of iterations. In addition, with an increase in the number of reflecting elements on RISs and the number of users, higher achievable SSR can be obtained.

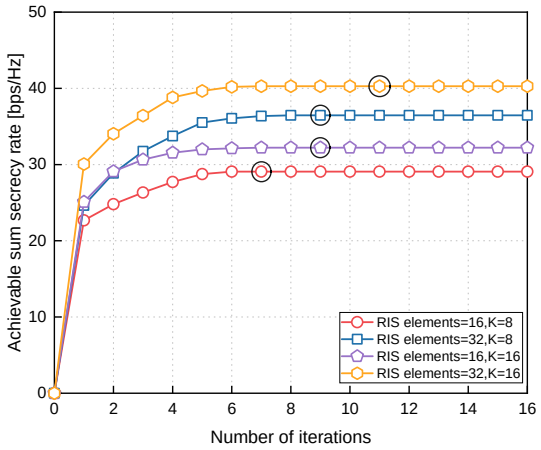

Fig. 2. Convergence of the proposed **Algorithm 2**.

C. Security Performance Evaluation

We evaluate the system security performance of the proposed **Algorithm 2** with the following baselines:

- **Baseline 1** (SBF + SUA): The secure beamforming (SBF), namely TBF at BSs and PBF at RISs are optimized based on algorithm in [36] and secure BSs-users association matrix is optimized by our proposed algorithm. This baseline is to demonstrate the effectiveness of the proposed secure beamforming (PSBF) algorithm.
- **Baseline 2** (PSBF + NDUA): TBF at BSs and PBF at RISs are optimized by PSBF and the nearest-distance-based BSs-users association (NDUA) algorithm is utilized to obtain association matrix. This baseline is to validate the the effectiveness of the proposed secure BSs-users association algorithm.
- **Baseline 3** (Random + NDUA): RISs are deployed and the phase shifts are randomly selected from $\mathcal{F}$. The NDUA algorithm is utilized to obtain association matrix and the proposed TBF optimization algorithm is applied. This baseline is to indicate the importance of properly optimizing RIS phase shifts.
- **Baseline 4** (NoRIS + NDUA): We assume RISs are not deployed in the system and the NDUA algorithm is adopted to associate BSs with users. Moreover, TBF matrix at each BS is optimized based on our proposed algorithm. This baseline is to show the PLS enhancement brought by RISs and secure BSs-users association.
- **Baseline 5** (NoRIS + RSUA): BSs-users association is acquired based on received signal strength (RSUA) [24] at each user, others are the same as Baseline 4.

Besides, the security performance between continuous and discrete RISs phases shifts are also compared in results. The following security performance results are acquired by averaging over 200 independent channel generations with different users locations.

The relationship between system SSR and the transmit power at each BS is illustrated in Fig.3. When the transmit power is low, the performance between all baselines is comparable. As the transmit power increases, the achievable SSR of all schemes gradually increases. From the results, it can be observed that the discrete phase shifts ($b = 3$) results of RISs are very close to the continuous phase shifts results for the proposed algorithm, which implies that the proposed algorithm can effectively handle the discrete phase scenario of RISs. Compared with other baselines, the proposed algorithm can achieve the highest SSR, especially compared to baseline 4 without RISs in system (166.1% SSR enhancement). The increase in transmit power enhances the communication rate for legitimate users, but it also leads to an increase in eavesdroppers' wiretapping rate. By jointly optimizing phases shifts of RISs and secure BSs-users association, baseline 1 and the proposed algorithm can efficiently utilize the limited power to handle the signal leakage, which contributes to higher SSR. Since NDUA in baseline 2 only considers the distance between users and BSs, ignoring the presence of eavesdroppers, its performance is inferior to the proposed algorithm based on SUA. For baseline 3, RISs phase shifts are randomly selected and the interaction between PBF and BSs-users association is not fully exploited. As for baseline 4 and baseline 5, the improvement of SSR is mainly due to the optimization of beamforming at each BS, where the potential of RISs in signal aggregation and user association is not fully utilized.

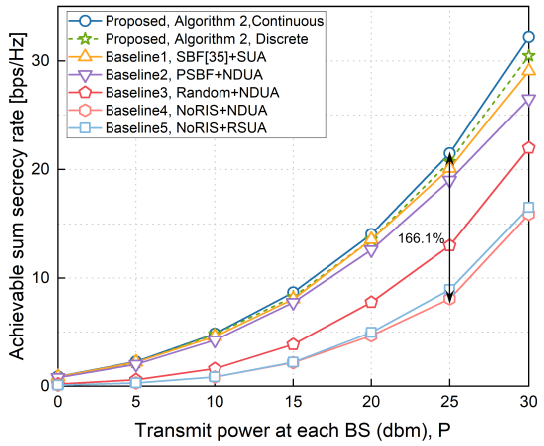

Fig. 3. Achievable SSR versus transmit power at each BS, $K = 16$

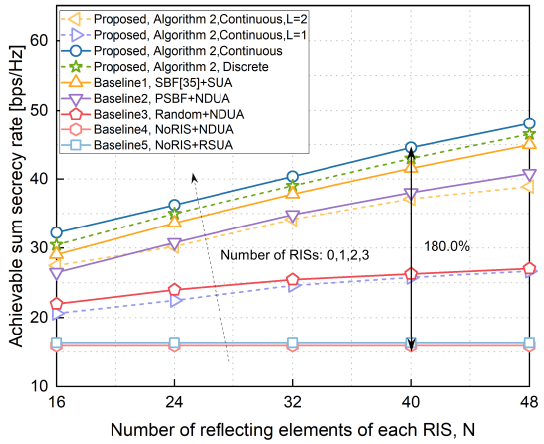

Fig. 4. Achievable SSR versus number of reflecting elements at each RIS, $K = 16$

The security performance of achievable SSR versus number

of reflecting elements at each RIS is shown in Fig.4. With the increase of the number of passive reflecting elements at each RIS, the achievable SSR gradually increases as well. Since more reflecting elements enable RIS to receive more signal from assisted-BS and reflect more effective signal to served legitimate users, communication rate of users can be greatly boosted, which is in alignment with baseline1, baseline2 and the proposed algorithm. However, malicious eavesdroppers can also benefit from RIS to enhance the wiretapping rate. From baseline3, we can figure out merely increasing the number of reflecting elements on RISs without considering the utilization of RIS to suppress eavesdropping behavior (PBF) leads to slight improvement in the security performance. The reason why the proposed algorithm can achieve fabulous security performance (e.g., 180% SSR enhancement) with the increasing number of RISs elements can be primarily attributed to two factors. On one hand, by carefully designing the phase shifts of RISs, the signal can be effectively focused and directed towards legitimate users (with a greater number of reflecting elements yielding more pronounced effects), thereby limiting eavesdroppers' ability to intercept the signal. On the other hand, RISs can extend the coverage of the incident signal, providing more possibilities for BSs to select users strategically and minimize the impact of eavesdroppers, which enables the proposed secure BSs-users association algorithm to be more flexible and achieve better results. Furthermore, Fig.4 also compares the achievable SSR under different numbers of deployed RISs. It can be observed that increasing the number of RISs leads to a higher SSR, as more spatial resources and signal reconfigurability enhance the system's ability to suppress information leakage and improve secure transmission.

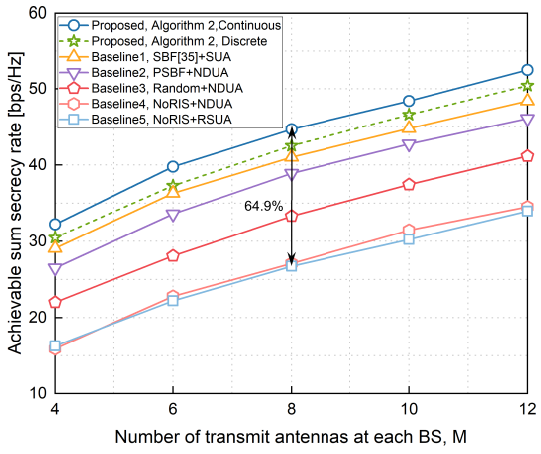

Fig. 5. Achievable SSR versus the number of transmit antennas at each BS, $K = 16$

As shown in Fig.5, we plot the security performance of achievable SSR versus number of transmit antennas at each BS. It can be observed that as the number of antennas at each BS increases, the achievable SSR for all schemes gradually increases since more degrees of freedom is introduced. Besides, the proposed algorithm outperforms other baselines, e.g. 64.9% SSR improvement.

We also plot the security performance of achievable SSR versus number of legitimate users in Fig.6, which indicates that achievable SSR gradually increases as the number of legitimate users increases. And the performance of the proposed algorithm is better than other baselines, especially when no RIS is deployment (baseline 4 and baselin 5), e.g. 153.8% SSR enhancement. This contributes to the joint design of secure active beamforming at BSs, passive beamforming at RISs and the secure BSs-users association matrix for limiting the eavesdroppers' wiretapping behavior. Furthermore, it can be observed that as the number of users in the system increases to a certain threshold ($K = 20$), the speed at which the achievable SSR increases slows down. This is because the communication capacity of the system is limited and the interference between users also increases with more users. With limited resources such as transmit power and antennas number, BSs cannot infinitely increase the communication rate for serving users and guarantee secure communication for each user, thus restricting the SSR improvement.

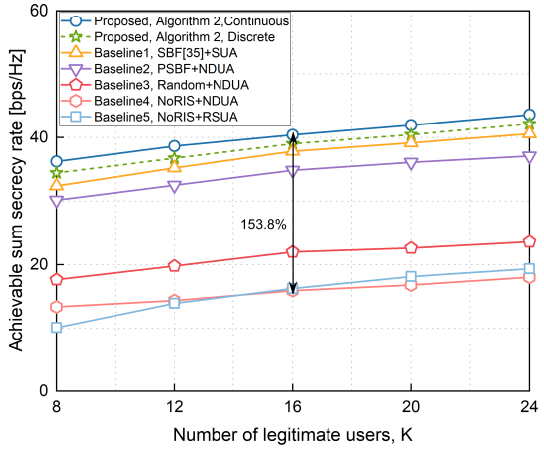

Fig. 6. Achievable SSR versus number of legitimate users, $N = 32$

Furthermore, to visually demonstrate the effectiveness of the proposed algorithm in reducing signal leakage and providing users with high SR as much as possible, we plot the average number of users at various SR thresholds (the higher SR means BS and user can achieve secure communication with the higher communication rate) in Fig.7. Under various threshold settings, the proposed algorithm outperforms other baselines, especially when the SR threshold is large. The results clearly indicate that by deploying RISs strategically and jointly optimizing RISs phase shifts and secure BSs-users association, significant improvements in SR can be achieved for users (compared to baseline 4 and baseline 5). As for BSs-users association based on NDUA algorithm (baseline 2 and baseline 3), the allocation of BSs to users is determined solely based on the proximity without considering the threat posed by the eavesdroppers and RISs benefit. In comparison, the proposed secure BSs-users association based on auction algorithm comprehensively takes into account the behavior of eavesdroppers and exploit the coverage possibility brought by RISs during the BSs-users matching process to ensure secure communication for as many users as possible, resulting in better security performance.

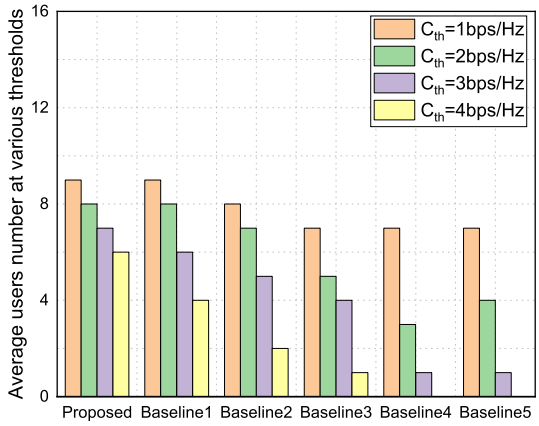

Fig. 7. Average number of users at various thresholds, $K = 16$

V. Conclusion

In this paper, we focus on a multi-RIS-assisted multi-BS and multi-user wiretap system with malicious eavesdroppers in hotspots. Due to the signal coverage enhancement brought by RISs, the PBF at RISs and the secure BSs-users association are considered together. To alleviate the impact of the signal leakage caused by eavesdroppers, we formulate a SSR maximization problem based on secure BSs-users association. The alternating optimization method is adopted to decompose the formulated non-convex problem into three subproblems. Further, we efficiently optimize the TBF at BSs with SCA and SDR methods. And the PBF at RISs is optimized based on quadratic transform method with each element of RIS is iteratively acquired with other elements fixed. Besides, the secure BSs-users association optimization subproblem is handled by the proposed two-step auction algorithm. Simulation results verify that the proposed algorithm outperforms baselines in achieving higher system SSR and SR at each user.

In the future, four aspects of expansion can be considered. On one side, the imperfect even unknown CSI of the eavesdropper should be investigated since the eavesdropper may avoid exchanging CSI with BSs, which increases the difficulty of channel estimation. Hence, more robust algorithms should be proposed to handle the challenge brought by channel estimation errors. On the other side, further consideration can be given to multi-objective system design, such as improving user fairness while ensuring security and maintaining energy efficiency. This requires the development of algorithms capable of balancing security performance, fairness, and energy consumption in large-scale deployments. Moreover, future work could explore the application of advanced RIS architectures such as active simultaneously transmitting and reflecting RIS (STAR-RIS) [45], which combines the simultaneous transmission and reflection capability of STAR-RIS with the signal amplification ability of active RIS. This hybrid design enables full-space coverage while mitigating the double-fading effect, potentially leading to improved secrecy performance and broader applicability in multi-BS secure communication systems. In addition, extending the current model to scenarios with multiple or cooperative eavesdroppers around each BS would be a meaningful direction, enabling a more comprehensive evaluation of secrecy performance in practical and complex environments.

Appendix I
Proof of Proposition 2

To demonstrate that the optimal $\mathbf{W}_{s,k}^{(t)}$ for BS s is a rank-one matrix, we need to analyze the KKT (Karush-Kuhn-Tucker) conditions of problem (26). Similar to [44], we first rewrite problem (26) removing rank-one constraint as follows:

$$\min_{\mathbf{W}_s^{(t)},a_k,b_k,u} \quad u \tag{55a}$$

$$s.t. \quad \bar{C}_{1,k} + \bar{C}_{2,k} - \bar{C}_{3,k} - \bar{C}_{4,k} \le u, \tag{55b}$$

$$a_k \ge \sum_{j\in\mathcal{U}(s)} \mathrm{Tr}(\mathbf{W}_{s,j}^{(t)}\mathbf{h}_{s,k}\mathbf{h}_{s,k}^H), \tag{55c}$$

$$b_k \ge \sum_{j\ne k}^{\mathcal{U}(s)} \mathrm{Tr}(\mathbf{W}_{s,j}^{(t)}\mathbf{h}_{s,e}\mathbf{h}_{s,e}^H), \tag{55d}$$

$$(26b), (26c) \tag{55e}$$

where $\bar{C}_{i,k}(i \in \{1,2,3,4\})$ are respectively given by

$$\bar{C}_{1,k} = -\sum_{k\in\mathcal{U}(s)} \log_2(a_k + \sigma_u^2), \tag{56a}$$

$$\bar{C}_{2,k} = -\sum_{k\in\mathcal{U}(s)} \log_2(b_k + \sigma_e^2), \tag{56b}$$

$$\bar{C}_{3,k} = -\sum_{k\in\mathcal{U}(s)} C_{3,k}^{(t)}\left(\mathbf{W}_s^{(t)}, \mathbf{W}_s^{(t-1)}\right), \tag{56c}$$

$$\bar{C}_{4,k} = -\sum_{k\in\mathcal{U}(s)} C_{4,k}^{(t)}\left(\mathbf{W}_s^{(t)}, \mathbf{W}_s^{(t-1)}\right), \tag{56d}$$

and a_k, b_k, u are introduced auxiliary variables. Then the Lagrangian function of problem (55) with respect to $\mathbf{W}_{s,k}^{(t)}$ for the k-th user can be obtained by (ignoring irrelevant terms)

$$\begin{aligned}\mathcal{L} = {} & \lambda\mathrm{Tr}(\mathbf{W}_{s,k}^{(t)}) - \mathrm{Tr}(\mathbf{W}_{s,k}^{(t)}\mathbf{G}_k) \\ & + \mu\sum_{j\in\mathcal{U}(s)} \mathrm{Tr}(\mathbf{W}_{s,j}^{(t)}\mathbf{h}_{s,e}\mathbf{h}_{s,e}^H) - \tau_k\sum_{j\in\mathcal{U}(s)} \mathrm{Tr}(\mathbf{W}_{s,j}^{(t)}\mathbf{h}_{s,k}\mathbf{h}_{s,k}^H),\end{aligned} \tag{57}$$

where λ, μ, τ_k and $\mathbf{G}_k$ are introduced Lagrange multipliers with respect to constraints (26b), (55b), (55c) and (26c), respectively. Further, KKT conditions regarding $\mathbf{W}_{s,k}^{(t)}$ can be expressed by

$$\lambda^*, \mu^*, \tau_k^* \ge 0, \mathbf{G}_k^* \succeq \mathbf{0}, \mathbf{G}_k^*\mathbf{W}_{s,k}^{(t)*} = \mathbf{0}, \nabla_{\mathbf{W}_{s,k}^{(t)}}\mathcal{L} = \mathbf{0} \tag{58}$$

We then acquire the partial derivative of (57) with respect to $\mathbf{W}_{s,k}^{(t)}$ and apply KKT conditions

$$\nabla_{\mathbf{W}_{s,k}^{(t)}}\mathcal{L} = \lambda^*\mathbf{I}_M - \mathbf{G}_k^* + \mu^*\mathbf{h}_{s,e}\mathbf{h}_{s,e}^H - \tau_k^*\mathbf{h}_{s,k}\mathbf{h}_{s,k}^H \tag{59}$$

Let $\nabla_{\mathbf{W}_{s,k}^{(t)}} = \mathbf{0}$ and $\mathbf{A} = \mu^*\mathbf{h}_{s,e}\mathbf{h}_{s,e}^H - \tau_k^*\mathbf{h}_{s,k}\mathbf{h}_{s,k}^H$ is a Hermitian matrix, then we have $\mathbf{G}_k^* = \lambda^*\mathbf{I}_M - \mathbf{A}$. We define $\lambda_{\mathbf{A}}^{\max}$ as the maximum eigenvalue of $\mathbf{A}$. Since $\mathbf{G}_k^* \succeq \mathbf{0}$ is required in (58), we have $\lambda^* \ge \lambda_{\mathbf{A}}^{\max} \ge 0$. Due to the condition $\mathbf{G}_k^*\mathbf{W}_{s,k}^{(t)*} = \mathbf{0}$, if $\lambda^* > \lambda_{\mathbf{A}}^{\max}$, $\mathbf{G}_k^*$ will be full rank, which indicating $\mathbf{W}_{s,k}^{(t)*} = \mathbf{0}$. Obviously, this is not the optimal solution satisfying the non-negative requirement of SR. For $\lambda^* = \lambda_{\mathbf{A}}^{\max}$, we have $\mathrm{rank}(\mathbf{G}_k^*) = M - 1$ then $\mathbf{W}_{s,k}^{(t)*}$ is a rank-one matrix, which completes the proof.

REFERENCES

[1] W. Saad, M. Bennis and M. Chen, "A vision of 6G wireless systems: Applications, trends, technologies, and open research problems," *IEEE Netw.*, vol. 34, no. 3, pp. 134-142, May 2020.

[2] Z. Lin, G. Qu, X. Chen and K. Huang, "Split learning in 6G edge networks," *IEEE Wireless Commun.*, vol. 31, no. 4, pp. 170–176, Aug. 2024,

[3] A. Almohamad et al., "Smart and secure wireless communications via reflecting intelligent surfaces: A short survey," *IEEE Open J. Commun. Soc.*, vol. 1, pp. 1442-1456, 2020.

[4] Q. Wu and R. Zhang, "Towards smart and reconfigurable environment: Intelligent reflecting surface aided wireless network," *IEEE Commun. Mag.*, vol. 58, no. 1, pp. 106-112, Jan. 2020.

[5] Q. Wu and R. Zhang, "Intelligent reflecting surface enhanced wireless network via joint active and passive beamforming," *IEEE Trans. Wireless Commun.*, vol. 18, no. 11, pp. 5394-5409, Nov. 2019.

[6] C. Huang, A. Zappone, G. C. Alexandropoulos, M. Debbah and C. Yuen, "Reconfigurable intelligent surfaces for energy efficiency in wireless communication," *IEEE Trans. Wireless Commun.*, vol. 18, no. 8, pp. 4157-4170, Aug. 2019.

[7] A. K. Papazafeiropoulos, C. Pan, P. Kourtessis, S. Chatzinotas, and J. M. Senior, "Intelligent reflecting surface-assisted MU-MISO systems with imperfect hardware: Channel estimation and beamforming design," *IEEE Trans. Wireless Commun.*, vol. 21, no. 3, pp. 2077–2092, 2022.

[8] S. H. Hong, J. Park, S. -J. Kim and J. Choi, "Hybrid beamforming for intelligent reflecting surface aided millimeter wave MIMO systems," *IEEE Trans. Wireless Commun.*, vol. 21, no. 9, pp. 7343-7357, Sept. 2022.

[9] B. Zhang, K. Xu, X. Xia, G. Hu, C. Wei, C. Li, and K. Cheng, "Sum-rate enhancement for RIS-assisted movable antenna systems: Joint transmit beamforming, reflecting design, and antenna positioning," *IEEE Trans. Veh. Technol.*, vol. 74, no. 3, pp. 4376–4392, 2025.

[10] G. Zhang, Y. Lu, L. Zhu, W. Chen, Z. Zhong and T. Q. S. Quek, "Hybrid beamforming design for RIS-aided full-duplex cell-free networks," *IEEE Trans. Commun.*, early access, 2025.

[11] W. Mao, Y. Lu, C.-Y. Chi, B. Ai, Z. Zhong, and Z. Ding, "Communication-sensing region for cell-free massive MIMO ISAC systems," *IEEE Trans. Wireless Commun.*, vol. 23, no. 9, pp. 12396–12410, Sept. 2024.

[12] B. Chong, H. Lu, L. Qin, C. Zhang, J. Li and C. W. Chen, "Power optimization in multi-IRS aided delay-constrained IoVT systems," *IEEE Trans. Veh. Technol.*, vol. 74, no. 1, pp. 1020-1034, Jan. 2025.

[13] M. Cui, G. Zhang and R. Zhang, "Secure wireless communication via intelligent reflecting surface," *IEEE Wireless Commun. Lett.*, vol. 8, no. 5, pp. 1410-1414, Oct. 2019.

[14] X. Guan, Q. Wu and R. Zhang, "Intelligent reflecting surface assisted secrecy communication: Is artificial noise helpful or not?" *IEEE Wireless Commun. Lett.*, vol. 9, no. 6, pp. 778-782, Jun. 2020.

[15] J. Chen, Y.-C. Liang, Y. Pei and H. Guo, "Intelligent reflecting surface: A programmable wireless environment for physical layer security," *IEEE Access*, vol. 7, pp. 82599-82612, Jun. 2019.

[16] X. Yu, D. Xu, Y. Sun, D. W. K. Ng and R. Schober, "Robust and secure wireless communications via intelligent reflecting surfaces," *IEEE J. Sel. Areas Commun.*, vol. 38, no. 11, pp. 2637-2652, Nov. 2020.

[17] S. Hong, C. Pan, H. Ren, K. Wang and A. Nallanathan, "Artificial-noise-aided secure MIMO wireless communications via intelligent reflecting surface," *IEEE Trans. Commun.*, vol. 68, no. 12, pp. 7851-7866, Dec. 2020.

[18] L. Dong and H.-M. Wang, "Enhancing secure MIMO transmission via intelligent reflecting surface," *IEEE Trans. Wireless Commun.*, vol. 19, no. 11, pp. 7543-7556, Nov. 2020.

[19] W. Jiang, B. Chen, J. Zhao, Z. Xiong and Z. Ding, "Joint active and passive beamforming design for the IRS-assisted MIMOME-OFDM secure communications," *IEEE Trans. Veh. Technol.*, vol. 70, no. 10, pp. 10369-10381, Oct. 2021.

[20] X. Pang, N. Zhao, J. Tang, C. Wu, D. Niyato and K. -K. Wong, "IRS-assisted secure UAV transmission via joint trajectory and beamforming design," *IEEE Trans. Commun.*, vol. 70, no. 2, pp. 1140-1152, Feb. 2022.

[21] Q. Liu, Y. Zhu, M. Li, R. Liu, Y. Liu and Z. Lu, "DRL-based secrecy rate optimization for RIS-assisted secure ISAC systems," *IEEE Trans. Veh. Technol.*, vol. 72, no. 12, pp. 16871-16875, Dec. 2023.

[22] Z. Wang, W. Wu, F. Zhou et al., "IRS-enhanced spectrum sensing and secure transmission in cognitive radio networks," *IEEE Trans. Wireless Commun.*, vol. 23, no. 8, pp. 10271–10286, Aug. 2024.

[23] J. Lei, X. Mu, T. Zhang and Y. Liu, "RIS assisted near-field NOMA communications: A security-fairness trade-off," *IEEE Trans. Veh. Technol.*, early access, 2025.

[24] D. Liu et al., "User association in 5G networks: A survey and an outlook," *IEEE Commun. Surveys Tuts.*, vol. 18, no. 2, pp. 1018-1044, 2nd Quart. 2016.

[25] F. Guo, H. Lu, D. Zhu, and Z. Gu, "Joint user association, grouping and power allocation in uplink NOMA systems with QoS constraints," in *Proc. IEEE Int. Conf. Commun. (ICC)*, May 2019, pp. 1–6.

[26] F. Fang, G. Ye, H. Zhang, J. Cheng and V. C. M. Leung, "Energy-efficient joint user association and power allocation in a heterogeneous network," *IEEE Trans. Wireless Commun.*, vol. 19, no. 11, pp. 7008-7020, Nov. 2020.

[27] W. Mei and R. Zhang, "Performance analysis and user association optimization for wireless network aided by multiple intelligent reflecting surfaces," *IEEE Trans. Commun.*, vol. 69, no. 9, pp. 6296-6312, Sept. 2021.

[28] D. Zhao, H. Lu, Y. Wang, H. Sun and Y. Gui, "Joint power allocation and user association optimization for IRS-assisted mmWave systems," *IEEE Trans. Wireless Commun.*, vol. 21, no. 1, pp. 577-590, Jan. 2022.

[29] J. Mirza and B. Ali, "Channel estimation method and phase shift design for reconfigurable intelligent surface assisted MIMO networks," *IEEE Trans. Cogn. Commun. Netw.*, vol. 7, pp. 441–451, Apr. 2021.

[30] L. Wei et al., "Channel estimation for RIS-empowered multi-user MISO wireless communications," *IEEE Trans. Commun.*, vol. 69, no. 6, pp. 4144-4157, Jun. 2021.

[31] Y. Wang, H. Lu and H. Sun, "Channel estimation in IRS-enhanced mmWave system with super-resolution network," *IEEE Commun. Lett.*, vol. 25, no. 8, pp. 2599-2603, Aug. 2021.

[32] Y. Guo et al., "Efficient channel estimation for RIS-aided MIMO communications with unitary approximate message passing," *IEEE Trans. Wireless Commun.*, vol. 22, no. 2, pp. 1403-1416, Feb. 2023.

[33] W. Cai, R. Liu, M. Li, Y. Liu, Q. Wu and Q. Liu, "IRS-assisted multicell multiband systems: Practical reflection model and joint beamforming design," *IEEE Trans. Commun.*, vol. 70, no. 6, pp. 3897-3911, Jun. 2022.

[34] A. Alvarado, G. Scutari, and J.-S. Pang, "A new decomposition method for multiuser DC-programming and its applications," *IEEE Trans. Signal Process.*, vol. 62, no. 11, pp. 2984–2998, 2014.

[35] M. Razaviyayn, "Successive convex approximation: Analysis and applications," Ph.D. dissertation, Univ. of Minnesota, Minneapolis, MN, USA, 2014.

[36] J. Li, L. Zhang, K. Xue, Y. Fang and Q. Sun, "Secure transmission by leveraging multiple intelligent reflecting surfaces in MISO systems," *IEEE Trans. Mobile Comput.*, vol. 22, no. 4, pp. 2387-2401, Apr. 2023.

[37] R. Feng, Q. Li, Q. Zhang and J. Qin, "Robust secure beamforming in MISO full-duplex two-way secure communications," *IEEE Trans. Veh. Technol.*, vol. 65, no. 1, pp. 408-414, Jan. 2016.

[38] H. Fu, S. Feng, W. Tang and D. W. K. Ng,"Robust secure beamforming design for two-user downlink MISO rate-splitting systems," *IEEE Trans. Wireless Commun.*, vol. 19, no. 12, pp. 8351-8365, Dec. 2020.

[39] A. A. Nasir, H. D. Tuan, T. Q. Duong, and H. V. Poor, "Secrecy rate beamforming for multicell networks with information and energy harvesting," *IEEE Trans. Signal Process.*, vol. 65, no. 3, pp. 677–689, Feb. 2017.

[40] H. Niu et al., "Joint beamforming design for secure RIS-assisted IoT networks," *IEEE Internet Things J.*, vol. 10, no. 2, pp. 1628–1641, Jan. 2023.

[41] H. Guo, Y. -C. Liang, J. Chen and E. G. Larsson, "Weighted sum-rate maximization for intelligent reflecting surface enhanced wireless networks," in *Proc. IEEE Global Commun. Conf. (GLOBECOM)*, Waikoloa, HI, USA, 2019, pp. 1-6.

[42] D. P. Bertsekas, *Network Optimization: Continuous and Discrete Models*. Belmont, MA, USA: Athena Scientific, 1998.

[43] G. Athanasiou, P. C. Weeraddana, and C. Fischione, "Auction-based resource allocation in millimeter wave wireless access networks," *IEEE Commun. Lett.*, vol. 17, no. 11, pp. 2108–2111, Nov. 2013.

[44] D. Xu, X. Yu, Y. Sun, D. W. K. Ng, and R. Schober, "Resource allocation for secure IRS-assisted multiuser MISO systems," in *Proc. IEEE Globecom Workshops*, Dec. 2019, pp. 1–6.

[45] A. Papazafeiropoulos, H. Ge, P. Kourtessis, T. Ratnarajah, S. Chatzinotas, and S. Papavassiliou, "Two-timescale design for active STAR-RIS aided massive MIMO systems," *IEEE Trans. Veh. Technol.*, vol. 73, no. 7, pp. 10118–10134, Jul. 2024.